Bulletin of the Geological Society of Finland, Vol. 91, 2019, pp 5–33, https://doi.org/10.17741/bgsf/91.1.001

# Tracing the styles of mafic-felsic magma interaction: A case study from the Ahvenisto igneous complex, Finland

Riikka Fred[1*], Aku Heinonen[1] and Pasi Heikkilä[1,2]

[1] *Department of Geosciences and Geography, PO Box 64, FI-00014, University of Helsinki, Finland*

[2] *Geological Survey of Finland, PO Box 96, FI-02151 Espoo, Finland*

VERTAISARVIOITU
KOLLEGIALT GRANSKAD
PEER-REVIEWED
www.tsv.fi/tunnus

## Abstract

The 1.64 Ga Ahvenisto complex, southeastern Finland, is an anorthosite-mangerite-charnokite-granite (AMCG) suite in which diverse interaction styles of coeval mafic and felsic magmas are observed. Commingling, resulting in mafic pillows and net-veined granite dykes, and chemical mixing producing hybrid rocks, are the most common interaction types. Detailed description of the factors that controlled the interaction styles and relationships between involved rock types are provided using targeted mapping, petrography, and geochemical analyses complemented by chemical mixing and melt viscosity modeling. Interaction occurred at intermediate stages in the magmatic evolution of the complex: when the last fractions of mafic (monzodioritic) melts and the earliest fractions of felsic (hornblende granitic) melts existed simultaneously. Differentiation of mafic magma has produced three monzodioritic rock types: 1) olivine monzodiorite (most mafic, Mg# 49–40), 2) ferrodiorite (Mg# 42–33), and 3) massive monzodiorite (most evolved, Mg# 28–27). The types form an evolutionary trend, and each exhibits different style of interaction with coeval hbl-granite resulting from contrasting conditions and properties (temperature, viscosity, composition). The variation in these properties due to magma evolution and relative proportions of interacting magmas dictated the interaction style: interaction between olivine monzodiorites and granite was almost negligible; ferrodiorites intermingled forming pillows with granitic veins intruding them; and chemical mixing of massive monzodiorite and hbl-granite produced hybrid rocks.

Keywords: mingling, mixing, Ahvenisto complex, viscosity, model

*Corresponding author (e-mail: riikka.fred@helsinki.fi)

Editorial handling: Arto Luttinen (arto.luttinen@helsinki.fi)

# 1. Introduction

Intrusion of mafic mantle-derived magmas into the continental crust as a result of underplating or extensional tectonics often leads to generation of coeval granitic magmas via partial melting of the lower crust (Huppert & Sparks, 1988; Hall, 1996; Wiebe, 1996). Simultaneous existence and emplacement of these magmas with contrasting (mafic-felsic) chemical compositions allows them to interact at different depths of the magmatic system. Depending on conditions (e.g. pressure, temperature) and composition (e.g. silica and water content) this interaction may result in mingling or mixing or both (Huppert & Sparks, 1988; Wiebe, 1996) in the same magmatic system (Chapman & Rhodes, 1992; Wiebe, 1993; Katzir et al., 2007; Weidendorfer et al., 2014). Magmas with contrasting chemical compositions, viscosities, temperatures, and crystallinities are not able to chemically mix, which leads to intermingling and physical mixing: the magmas stay as separate phases or produce a heterogeneous magma (Sparks & Marshall, 1986). The development of the magma system may lead to a situation in which the contrasts diminish, and the magmas are also able to chemically mix, and produce a homogeneous hybrid magma (Walker & Skelhorn, 1966). Thus, mafic magmas are able to induce melting to produce felsic magmas, but coeval existence of these melts may further guide their chemical and thermal evolution (Wiebe, 1996).

Net-veined and mafic pillow structures are typical results of magma mingling, and in Figure 1, a representative example of these from the Ahvenisto complex in Finland is illustrated. In these structures, mafic magma forms irregular to regular pillows and felsic material intrudes them forming net-veined structures (Fig. 1). The numerous other known localities of this type of structures include Jaala-Iitti in Finland, Vinalhaven in Maine, Mullach Scar in St Kilda, Lamarck in Sierra Nevada, and Adamello in Italy (Marshall & Sparks, 1984; Frost & Mahood, 1987; Blundy & Sparks, 1992; Hibbard, 1995; Salonsaari, 1995; Wiebe, 1996; Wiebe et al., 2001).

The mechanisms that produce pillow-like mingling structures in bimodal magma systems have been studied extensively (e.g., Wiebe et al., 2001; Campos et al., 2011; Hodge et al., 2012; Hodge & Jellinek, 2012; Bain et al., 2013). The style of commingling and/or mixing depends on the order of the injection of the two magmas (Snyder & Tait, 1995; Snyder et al., 1997; Wiebe & Ulrich, 1997; Katzir et al., 2007; Litvinovsky et al., 2017). In dykes with mafic margins, the two magma types are usually arranged in parallel homogenous sheets, whereas in dykes with felsic margins the mafic magma often forms pillows (Snyder & Tait, 1995; Snyder et al., 1997). Based on this observation, it has been suggested that mafic pillows with felsic veining, are generally formed when a relatively denser and less viscous mafic magma intrudes an existing reservoir of felsic magma (Wiebe, 1993; Snyder & Tait, 1995; Wiebe et al., 2001).

In some cases mafic pillows show chilled margins against the felsic rocks (Walker & Skelhorn, 1966; Wiebe et al., 2001). Mafic pillows can for example have sharp lower contacts and diffusive upper contacts against the surrounding granites (Wiebe, 1991). Rapid crystallization of mafic pillows is also often indicated by clusters of skeletal plagioclase laths. Mafic pillows may also be sharply cut by thin veins of felsic material (apophyses), against which no chilled margins are observed (Walker & Skelhorn, 1966). Many of these features are controlled by heat exchange between the two compositionally contrasting magmas (Wiebe, 1993). Before chemical mixing and homogenization of two magmas can occur, they must reach thermal equilibrium (Sparks & Marshal, 1986), because changes in thermal equilibrium also lead to changes in relative rheological properties of the magmas. Therefore, if the felsic phase dominates, hybridization can only occur with relatively evolved mafic magmas (Sparks & Marshal, 1986). In general, mafic magma with basaltic composition must dominate in order for it to be able to mix with felsic magma. If thermal equilibrium is rapidly approached, reversals of relative viscosities may occur, which may cause the mafic magma


Figure 1. Sketch of typical mafic pillow and net-veined mingling structures from Pärnäjärvi area in the Ahvenisto complex, Finland (see also Electronic Appendix A for more details): 1) mafic magma forms variable sized (0.1–2 m wide) pillows of regular to irregular shapes, and 2) felsic magma intrude them forming net-veined structures (vein thickness usually 1–30 cm).

to solidify and the silicic magma to become superheated resulting in mingling structures (Blake et al., 1965).

Proterozoic AMCG (anorthosite-mangerite-charnokite-granite) complexes are bimodal (mafic-felsic) magmatic suites (Emslie, 1978, 1991; Ashwal, 1993; Alviola et al., 1999; Heinonen, 2012) in which different types of interactions of mafic and felsic magmas have been recognized as important petrogenetic processes. In the 1.64 Ga Ahvenisto rapakivi granite – massif-type anorthosite complex of southeastern Finland (Savolahti, 1956, 1966; Johanson, 1984; Alviola et al., 1999; Heinonen 2012; Heinonen et al., 2010b, 2015) interaction of coeval mafic and felsic magmas has led to both mingling and chemical mixing processes. U-Pb geochronology and field relations reveal that in Ahvenisto, most of the mafic rocks are older than the bulk of the granitic rocks (e.g. Alviola et al., 1999). It appears that the last mafic phase, which is represented by monzodioritic residual melts, is coeval with felsic magmas of the earliest granitic phase (hbl-granite melts). This has enabled diverse forms of magmatic interaction (Alviola et al., 1999; Heinonen et al., 2010a). Prominent mingling structures between the monzodioritic and granitic rocks have been reported in the form of mafic pillows and net-veined granites (Johanson, 1984; Alviola et al., 1999). The presence of associated hybrid rocks (Johanson, 1984) suggests that also chemical mixing has taken place at some point of the magmatic evolution of the complex. The aim of this study is to provide a detailed description of the mingling structures and of the different rock types involved in mixing/mingling processes using field observations, petrography, and geochemistry. The results are used to model chemical mixing and in melt viscosity calculations (Giordano et al., 2008) to examine the interaction of granitic and monzodioritic rocks in the Ahvenisto complex.

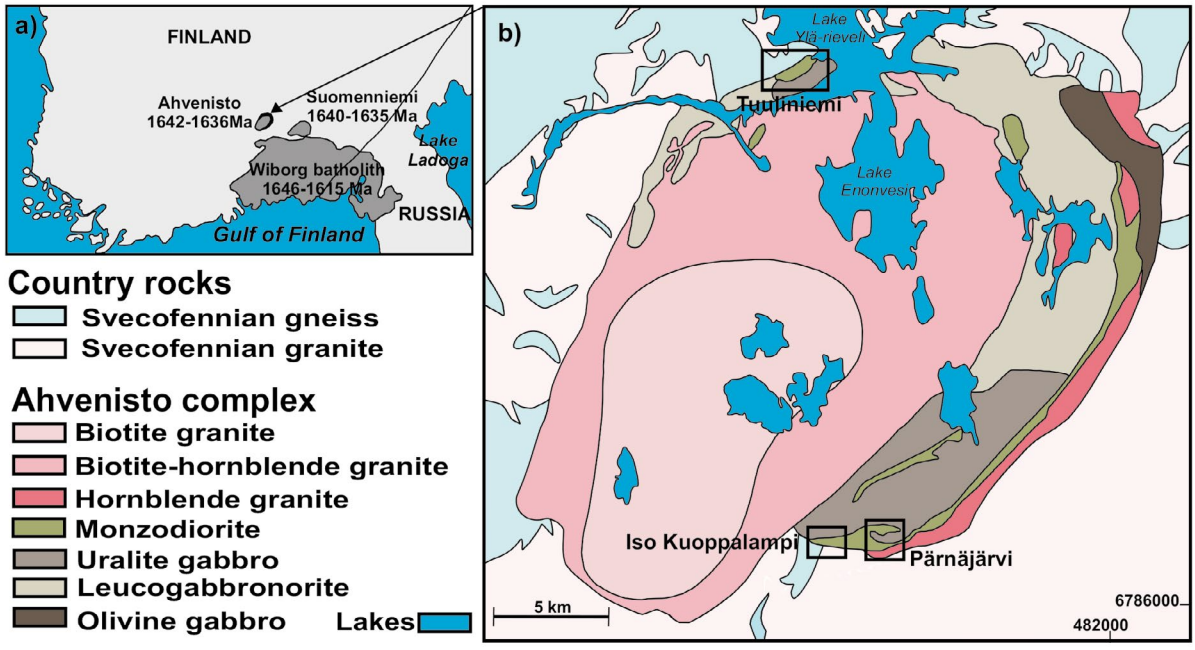


Figure 2. a) Map showing the location of the Ahvenisto complex northwest of the main Wiborg batholith and b) a simplified lithological map of the complex showing the main rock types. The three study areas are marked with black rectangles.

## 2. Geological background

The Ahvenisto complex is a part of the Wiborg rapakivi granite suite of southeastern Finland and adjacent Russia (Fig. 2a) and is one of the oldest plutons in the area, crystallized at 1643–1632 Ma (Alviola et al., 1999; Heinonen et al., 2010b). The Ahvenisto complex is located northwest of the main Wiborg batholith and represents a typical anorthosite-mangerite-charnokite-granite (AMCG) suite with diverse rock types ranging from massif-type gabbro-anorthositic rocks (cf. Ashwal, 1993) with minor monzodioritic rocks to rapakivi granites (Alviola et al., 1999; Heinonen et al., 2010a; Heinonen 2012). The felsic rocks are dominantly equigranular biotite and hbl-granites that form an oval intrusion partially rimmed by a horseshoe-shaped mafic arc in the east (Fig. 2b). The mafic arc contains leucogabbronorite, leuconorite, leucotroctolite, anorthosite, monzodiorite, and quartz-monzodiorite (Alviola et al., 1999; Heinonen et al., 2015). The Ahvenisto complex covers an area of ca. 350 km$^2$ and comprises 70 % felsic rocks, 25 % gabbro-anorthositic rocks, and 5 % monzodioritic rocks. The complex intruded Paleoproterozoic (ca. 1.80–1.93 Ga) Svecofennian crust with sharp contacts (Alviola et al., 1999) and according to field relations the felsic rocks are younger than any of the mafic rocks. Isotopic evidence suggests that the primary source of the mafic rocks was most likely asthenospheric depleted mantle and that the felsic rocks were derived from a Proterozoic lower crustal source (Heinonen et al., 2010a, 2010b, 2015). This indicates that the petrogenetic framework of the Ahvenisto complex is congruent with the classical two-source model (Emslie, 1978; Rämö & Haapala, 2005) rather than with the single-source models proposed for some other massif-type anorthositic complexes (Duchesne et al., 1999; Frost & Frost, 1997; see also Heinonen et al., 2010a). In Ahvenisto the mantle-derived mafic magma rose to the lower crust, and heat derived from its crystallization melted the crustal material, which produced the felsic magmas

(Emslie, 1978). This type of bimodal magmatic environment provides ample opportunities for diverse interaction of magmas with contrasting chemical compositions. Similar genesis has been suggested for massif-type anorthosites of the Nain complex in Labrador, Eastern Canada (Wiebe, 1987). Al-in-opx geobarometry (cf. Emslie et al., 1994) results show that the anorthositic and gabbroic rocks of Ahvenisto crystallized polybarically, at least at two, most likely at three depths in the crust: 1) at lower crustal high pressure conditions (up to 1.14 GPa, ~34 km) 2) at mid- to upper crust (0.53 GPa, ~20km), and 3) at the level of emplacement (0.19 GPa, <10km; Kivisaari, 2015).

Net-veined mingling structures between the granitic and the monzodioritic rocks are known from three locations in the Ahvenisto complex (Fig. 2b): two in the southern part of the mafic arc near lakes Pärnäjärvi and Iso Kuoppalampi, and one in the northwestern part of the complex in the Tuuliniemi area. Structurally the mingling structures are located between the anorthositic rocks and the Svecofennian country rocks in the northern Tuuliniemi area, and between the anorthositic rocks and a marginal hbl-granite in the southern study areas (Alviola et al., 1999). According to Heinonen et al. (2010b) the monzodioritic rocks represent the residual melt left after the fractional crystallization of the anorthositic rocks. The hbl-granite, which occurs outside of the gabbroic arc and separately from the main granite batholith, represents the earliest fraction of felsic melt, and the source of the granite veins in the mingling structures (Alviola et al., 1999).

# 3. Methods

## *3.1. Field work and sampling strategy*

Field work was focused on the previously known localities of pillow-structured rocks near lake Pärnäjärvi in the southern part of the complex (Alviola et al., 1999) and Tuuliniemi area in the north (Saku Vuori, pers. comm.; Johanson, 1984). A new locality of commingled rocks near the lake Iso Kuoppalampi (Fig. 3) was discovered in the southwestern tip of a monzodiorite ring dike. In addition to regional mapping, two detailed outcrop maps were drafted from Pärnäjärvi and Tuuliniemi in order to scrutinize the structural features of the mingling localities (Fig.1, Electronic Appendices A & B).

In total, eighteen samples were collected from the pillow structures (Fig. 3). The samples were chosen from different parts of the pillows to study their mineralogical and chemical variability within and between pillows. Three samples from the marginal hbl-granite in Pärnäjärvi and three from the leucocratic granite in Tuuliniemi were included as potential source rocks for the granitic veins. Three hybrid rock samples were collected to study the potential chemical mixing between mafic and felsic magmas.

## *3.2. Analytical techniques*

In total 33 sub-samples were prepared at the Department of Geosciences and Geography at the University of Helsinki for geochemical analysis and petrographic studies (Table 1). Thin sections were prepared at the Department of Geosciences and Geography and studied with polarized light microscope. The samples for XRF-analyses (x-ray fluorescence) were jaw-crushed into fragment size of 0.3–30 mm, wash sieved using a plastic sieve, rinsed with de-ionized water, and dried overnight in 105°C. About 30 g of representative fragments was hand-picked and powdered using a Fritch Pulverisette tungsten carbide ball mill at 350 rpm for 10+5 min. Glass beads for the XRF-analyses were prepared from 0.600 g ± 1 mg of sample and 6.000 g ± 1 mg of flux ($Li_2B_4O_7$ 49.75 % + $LiBO_2$ 49.75 % + LiBr 0.5 %). The powders were mixed and fused in 1000°C gas flame with a Claisse M4 fluxer using Pt-Au crucibles and molds (95% Pt, 5% Au). For XRD-analyses (x-ray diffraction), a small amount of sample powder was spread on a glass plate in acetone suspension and dried.

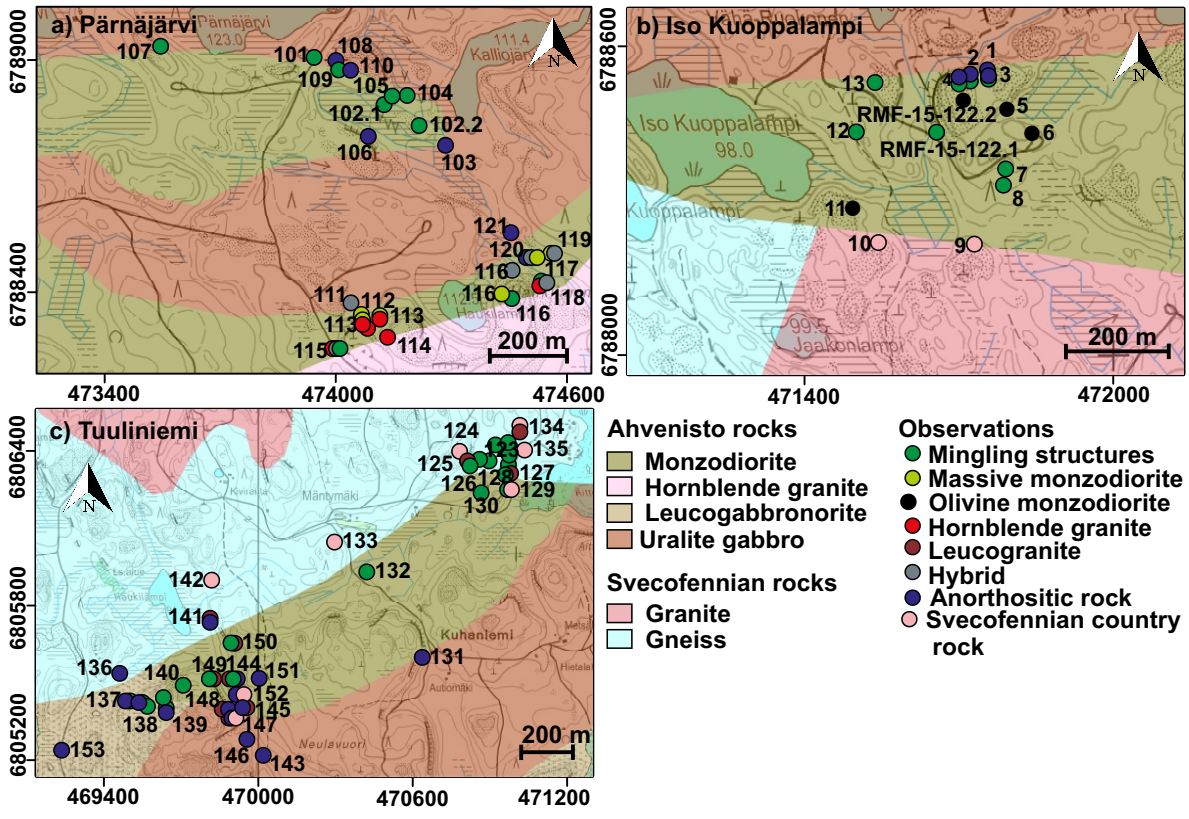


Figure 3. Field maps of the study areas a) Lake Pärnäjärvi, b) Iso Kuoppalampi, and c) Tuuliniemi with observation localities. DigiKP200 (GTK) and 1:100 000 large-scale topographical map (MML) were used as base maps. Coordinate grids are in ETRS-TM35FIN.

All samples were analyzed using wavelength dispersive X-ray fluorescence spectrometer (WD-XRF), PANalytical Axios mAX equipped with Rh-anode x-ray tube that was run at 3 kW power setting at the Department of Geosciences and Geography at the University of Helsinki. Major elements oxides and trace elements (Ba, Ce, Cu, Cr, La, Nb, Ni, Sr, Rb, U, V, Zn, Zr, Y) were calibrated using Certified Reference Material (CRM) rock powders that were fused into beads. The quantitative results were calculated using SuperQ 5.3 using fixed alpha theoretical matrix correction factors and selected line-overlap corrections. In the case of sixteen samples, the mineral assemblage was determined using PANalytical X'Pert 3 X-ray powder diffractometer at the Department of Geosciences and Geography. The diffractometer is based on Bragg-Brantagon geometry with theta-theta configuration, a Long Fine Focus (LFF) Cu line focus X-Ray tube, fixed sample holder, curved graphite monochromator and Xe-sealed gas proportional counter. The measurements were performed using the following instrument settings: 40 kV acceleration voltage, 40 mA current, 5.000–74.990 2-theta measurement range, 0.01°/s continuous scan speed, and a total measuring time of 1 h 57 min per sample. Identification of the mineral phases was done using the HighScorePlus-program that is linked to ICDD (*The International Centre for Diffraction Data*) PDF-4 *Minerals* -database.

Table 1. Documentation of the collected samples with a list of prepared subsamples for different analyses.

| Observation ID | Area | Collection method | Petrography/thin sections | Geochemistry | XRD-analyses |
|---|---|---|---|---|---|
| RMF-15-101 | 1 | Hammer | Contact 101-A.H1<br>Pillow 101-A.H2 | Pillow 101-A.X1 | Pillow 101-A.X1 |
| RMF-15-102/ APHE-14-011 | 1 | Saw | Granite 011.3.H1<br>Contact 011.5H1<br>Pillow 011.5.H2<br>Granite 011.5.H3<br>Granite 011.B.H1<br>Pillow 011.E.H1<br>Contact 011.F.H1<br>Pillow 011.F.H2 | Granite 011.3.X1<br>Granite 011.5.X1<br>Pillow 011.5.X2<br>Pillow 011.E.X1<br>Pillow rim 011.F.X2<br>Granite 011.F.X1 | Pillow 011.5.X2<br>Pillow 011.E.X1 |
| RMF-15-106 | 1 | Hammer | Anorthositic rock 106-A.H1 | Anorthositic rock<br>GM 106-A.X1.1<br>GM+Plg 106-A.X1.1 | |
| RMF-15-111 | 1 | Hammer | | Hybrid 111-A.X1 | Hybrid 111-A.X1 |
| RMF-15-112 | 1 | Hammer | Monzodioritic 112-A.H1 | Monzodiritic 112-A.X1 | Monzodiorite 112-A.X1 |
| RMF-15-114 | 1 | Hammer | Hbl-granite 114-A.H1 | Hbl-granite 114-A.X1 | |
| RMF-15-115 | 1 | Hammer | Contact 115-A.H1<br>Hbl-granite 115-B.H1<br>Hybrid 115-C.H1 | Hybrid 115-A.X1<br>Hbl-Granite 115-A.X2<br>Hbl-granite 115-B.X1<br>Hybrid 115-C.X1 | Hybrid 115-C.X1 |
| RMF-15-116 | 1 | Hammer | Hybrid 116-A.H1 | Hybrid 116-A.X1 | |
| RMF-15-123/ APHE-14-013 | 2 | Saw | Pillow 013.1.H1<br>Contact 013.1.H2<br>Granite 013.1.H3<br>Contact 013.A.H1<br>Pillow 013.B.H1<br>Contact 013.B.H2 | Pillow 013.1.X1<br>Red granite 013.1.X2<br>Pillow 013.1.X3<br>Pillow 013.1.X4<br>Granite 013.1.X5<br>Pillow 013.B.X1 | Pillow 013.1.X1<br>Pillow 013.1.X3<br>Pillow 013.1.X4<br>Pillow 013.B.X1 |
| RMF-15-125 | 2 | Hammer | Granite 125-A.H1 | Granite 125-A.X1 | |
| RMF-15-126 | 2 | Hammer | Contact 126-A.H1<br>Granite 126-A.H2<br>Pillow 126-A.H3 | Granite 126-A.X1<br>Pillow 126-A.X2 | Pillow 126-A.X2 |
| RMF-15-128 | 2 | Hammer | Granite 128-A.H1 | Granite 128-A.x1 | |
| RMF-15-129/ APHE-14-012 | 2 | Saw | Contact 012.1.H1<br>Pillow 012.1.H2 | Pillow 012.1.X2 | |
| RMF-15-136 | 2 | Hammer | Granite 136-A.H1 | Granite 136-A.X1 | |
| RMF-15-122 | 3 | Hammer | Mafic rock 122-A.H1 | Mafic rock 122-A.X1 | Mafic rock 122-A.X1 |
| APHE-16-5 | 3 | Hammer | | Mafic rock 5.X1 | Mafic rock 5.X1 |
| APHE-16-6 | 3 | Hammer | | Mafic rock 6.X1 | Mafic rock 6.X1 |
| APHE-16-11 | 3 | Hammer | | Mafic rock 11.X1 | Mafic rock 11.X1 |

# 4. Field observations

The interaction between mafic and granitic magmas at Ahvenisto complex has resulted in mingling structures and hybrid rock types generated by magma mixing: 1) pillow-like monzodiorite bodies intruded by thin granitic finger-like veins (Fig. 4a, b, e, & g), 2) massive monzodiorite (no pillows) with minor amounts of granitic material (Fig. 4f & h), and 3) hybrid rock types typified by potassium feldspar phenocrysts in a mafic groundmass (Fig. 4c). Near the contact of hbl-granite (Fig. 4d) and monzodiorite, complex interaction between the two magmas is observed; granite, monzodiorite, and hybrid rock occur together in pillows, cutting veins, and almost brecciating structures in which rock types grade from one to another in a rather random manner.

## *4.1. Lake Pärnäjärvi*

The monzodioritic ledge in Pärnäjärvi area (Fig. 3a) is characterized by monzodioritic pillows with intrusive granitic veins. Towards south the rock type relations become more complex containing pillow structures, hybrid rock, and massive monzodiorite. Locally, it is difficult to distinguish between the monzodioritic and hybrid rocks, because of gradational contacts.

The anorthositic rocks (usually uralite gabbro) of the lake Pärnäjärvi area are coarse-grained and light gray. They consist mainly of plagioclase (usually 1–2 cm) with minor interstitial mafic minerals (10–15 %). Their contact with the monzodioritic rocks is not exposed, but near the contact mingled monzodioritic rocks show distinct mingling characteristics: fine-grained, light red, leucocratic, finger-like granite veins intrude the monzodiorite (Fig. 4a). The monzodioritic pillows are fine- to medium-grained and consist of clusters of plagioclase laths and mafic minerals in dark gray groundmass (Fig. 4b). Potassium feldspar is not recognizable in hand samples. The contact with granite is irregular (Fig. 4b), locally diffuse, and associated with a dark 1–2 cm pillow rim (Fig 4b). In places granitic apophyses intrude the pillows with sharp contacts and no rim structures. The monzodiorite pillows are irregular in shape and range from a few centimeters up to two meters in diameter, whereas the thickness of granite veins is 0.1–20 cm (Electronic Appendices A and B, Fig. 4a, b, e & g).

Similar pillow structures are also observed next to the contact of the monzodiorite with the marginal hbl-granite (Fig. 3a). The hbl-granite has coarse-grained matrix and 1–2 cm potassium feldspar phenocrysts (Fig. 4d). Towards monzodiorite (Fig. 3a), the amount of granitic material decreases, and the monzodioritic material becomes more massive (no pillows), coarser and equigranular, and potassium feldspar is recognizable in hand samples. In places near the contact with the hbl-granite, the pillow structures grade into a hybrid rock (Fig. 4c). The contact of the monzodioritic rocks with the hbl-granite is in places complicated with pillow structures, granitic material, and hybrid rock occurring together: the granite intrudes both the monzodiorite and the hybrid rock, both of which form irregular pillows. The intruding granitic material is occasionally coarser and more mafic compared to vein granites on other outcrop localities.

## *4.2. Lake Iso Kuoppalampi*

A new mingling area was discovered near the lake Iso Kuoppalampi, ~2 km towards west of the Pärnäjärvi area, where monzodioritic rock forms pillow-like structures, and a leucocratic, fine-grained granite intrudes the pillows (Fig. 4e). The monzodioritic material in the pillows is fine-grained with clusters of plagioclase laths and mafic minerals. At the northern contact, the pillowed rocks are either in direct contact with the anorthositic rock, or there is a sheet of granite in between them. The southern contact area is more complex and the different rock types may grade into each other. Locally, the monzodioritic material grades into a mafic rock that is medium-grained and equigranular. The granitic material is absent or locally appears as inclusions


Figure 4. Outcrop photos of different rock types and styles of magma interaction observed in the Ahvenisto complex: a) and b) mingling of monzodiorite and granite from Pärnäjärvi; c) hybrid rock from Pärnäjärvi; d) hbl-granite intruding monzodiorite in Pärnäjärvi; e) mingling from Iso Kuoppalampi; f) olivine monzodiorite with a granite inclusion from Iso Kuoppalampi; g) mingling at Tuuliniemi; and h) massive monzodiorite from Tuuliniemi.

(Fig. 4f). Recent field work in 2018 revealed that the extent of the mingling structures is continuous between Pärnäjärvi and Iso Kuoppalampi, but the mafic rock only occurs as a small lens in the Iso Kuoppalampi area (Fig. 3b).

### 4.3. Tuuliniemi

The areal extent of the monzodioritic rocks in Tuuliniemi turned out to continue ~200 m further towards west from the presumed western contact of monzodiorite with leucogabbronorite (Fig. 3c). The mingling structures are concentrated close to the northern contact of monzodioritic rocks and are continuous throughout the width of the monzodioritic lens. A ca. 10 cm to 5 m thick, previously unreported leucogranite sheet was observed between the monzodioritic rocks and Svecofennian basement in the northern contact, in a structural position analogous to the marginal hbl-granite in Pärnäjärvi. The leucogranitic material in this sheet is fine-grained and appears similar to the granite in the mingling structures.

The pillow structures in Tuuliniemi (Fig. 4g) are similar to those observed in Pärnäjärvi with only minor differences: the amount and grain size of plagioclase laths in the pillows is smaller and also the mafic phenocrysts are smaller. The monzodioritic pillows are usually irregular in shape and their sizes range from 0.5 to 2 m (Electronic Appendix B, Fig. 4g). Granitic material is medium-grained and contains large quartz crystal clusters. The contacts are irregular, but somewhat sharper than at Pärnäjärvi. Recent field work in 2018 revealed that massive monzodiorite, located south of the mingling structures, is medium-grained and contains poikilitic hbl crystals (Fig. 4h).

The southern contact of the monzodioritic rocks in the southwestern end of the monzodioritic ledge is very complex. Between field observation RMF-15-144 and RMF-15-146 (Fig. 3c), monzodioritic, granitic, and anorthositic rocks with minor inclusions of country rock material are observed in a very irregular assemblage and different rock types grade into each other, similarly to Iso Kuoppalampi area. Locally, granite also brecciates anorthositic rocks and intrudes them as veins. It was not possible to resolve the structure in greater detail, but based on the existence of the Svecofennian host rock fragments the area might represent an internal upper or lower contact of the intrusion complex or an area rich in roof or base pendants.

## 5. Petrography

The following petrographic description is based on hand sample and thin section observations and supportive X-ray powder diffraction analysis of fine-grained samples. The full XRD data set is available in Electronic Appendix C.

### 5.1. Mafic rocks

Based on mineral composition, geochemical composition, and structural position, three different monzodioritic rock types were recognized in the study areas: 1) monzodioritic pillows, 2) massive monzodiorite, and 3) olivine-bearing monzodiorite.

The groundmass of the monzodioritic pillows in Pärnäjärvi consists of fine-grained plagioclase, chloritized biotite, quartz, and minor potassium feldspar. Mafic minerals are usually biotite and amphibole, but both minor clinopyroxene and orthopyroxene are also observed, as well as common accessory ilmenite. Plagioclase, amphibole, biotite, and in some samples pyroxene phenocrysts stand out from the groundmass (Fig. 5a). Near the contacts of the granitic veins, pyroxene is replaced by amphibole (colorless with very thin twinning lamellae). Plagioclase phenocrysts are partially skeletal and euhedral laths (0.5 to 10 mm) that show only minor sericitization, and usually form glomeroporphyritic clusters (Fig. 5a). Biotite and amphibole are often poikilitic. Biotite grain size ranges from small blebs to millimeter-sized flakes. Only scattered phenocrysts of green pleochroic amphibole are observed in the centers of the pillows, but they are more common in the contact zone. Rare fresh euhedral ortho- and clinopyroxene crystals (0.5–1 mm) are observed in the monzodioritic pillow centers.

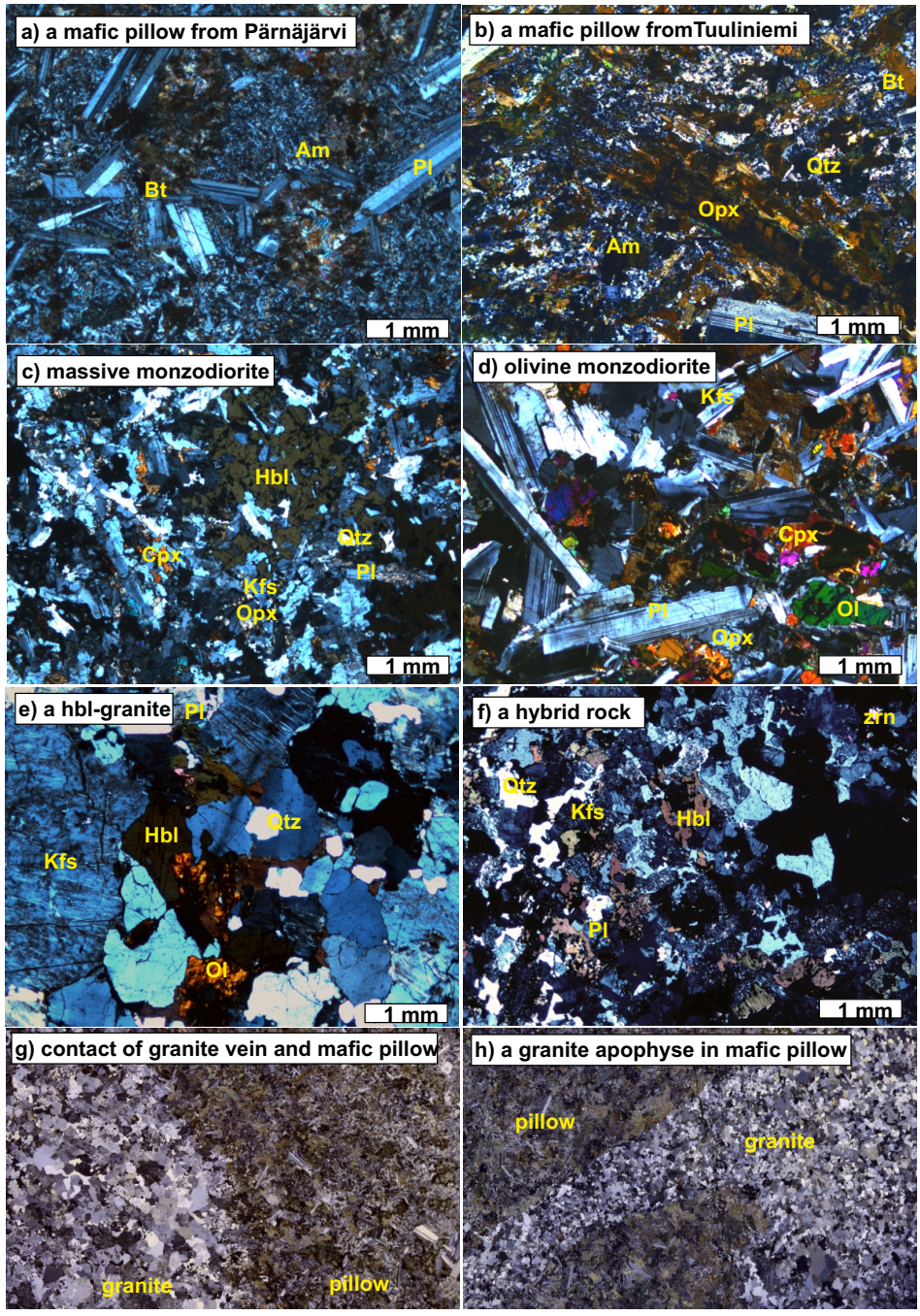


Figure 5. Photomicrographs of mafic pillow material from a) Pärnäjärvi and b) Tuuliniemi; c) massive monzodiorite from Pärnäjärvi; d) olivine monzodiorite from Pärnäjärvi; e) hbl-granite from Pärnärvi; f) hybrid rock from Pärnäjärvi. These figures outline the major mineralogical and textural differences of each rock type: plagioclase, biotite and amphibole phenocrysts in fine-grained groundmass in the pillows (a, b), poikilitic hornblende in coarser massive monzodiorite (c), olivine and pyroxenes in olivine monzodiorite (d), the more felsic nature of the hybrid rock (f), and the more mafic nature of the hbl-granite compared to vein granites (e, g, h). Photographs of entire thin sections show g) the slightly diffusive contacts between the pillows and the granitic veins, and h) a sharp contact against a late apophyse.

In Tuuliniemi, the pillows are mineralogically like those in Pärnäjärvi. The groundmass is somewhat coarser and more felsic, consisting of plagioclase, quartz, mafic minerals, and abundant ilmenite with minor amounts of potassium feldspar (Fig. 5b). Plagioclase, biotite, amphibole, and pyroxene phenocrysts are common. Amphibole pseudomorphs after pyroxenes are absent, and secondary amphibole is only observed in the groundmass. Plagioclase phenocrysts are euhedral and slightly skeletal with only minor sericitization and some mafic inclusions in the largest grains. The flaky biotite grains are often poikilitic. Green pleochroic amphibole is much more common than in Pärnäjärvi.

When the pillow structures become more scarce and the amount of granitic material decreases, the monzodiorite grades from the porphyritic towards equigranular, massive varieties. The content of pyroxenes increases, and biotite is typically associated with hornblende that is observed as poikilitic phenocrysts (Fig. 5c). Pyroxenes are anhedral, partially skeletal, and contain thin lamellae of opaque minerals. Plagioclase is euhedral and commonly twinned. Potassium feldspar is a major mineral in the massive monzodiorites.

The more mafic rock type observed in Iso Kuoppalampi area consists of plagioclase, orthopyroxene, clinopyroxene, olivine, and potassium feldspar with minor apatite, biotite, and ilmenite (Fig. 5d). Plagioclase is unaltered, and forms partially skeletal tabular grains, ranging from 0.3 to 1 mm. Olivine is fresh, euhedral, and usually rimmed by clinopyroxene. Both pyroxenes are present as subhedral crystals, some of which are strongly altered. Potassium feldspar is interstitial and forms symplectites with mafic minerals.

## 5.2. Granites

The hbl-granite in Pärnäjärvi is coarse-grained. Quartz seems to occur in two generations: euhedral quartz and anhedral interstitial quartz. Large potassium feldspar crystals (~4 mm) are anhedral, slightly perthitic, and sericitisized. Plagioclase is euhedral and strongly altered. The main mafic phase is hornblende that occurs together with minor olivine and biotite (Fig. 5e). Olivine occurs mainly within euhedral hornblende crystals and is almost completely altered to iddingsite. Accessory amounts of zircon also occur within hornblende.

The fine- and even-grained granites in the finger-like veins in Pärnäjärvi are leucocratic with biotite as the only mafic phase. Granophyric textures are common especially near the contacts with the pillows (Fig. 5g & h). Anhedral potassium feldspar is the dominant feldspar and most of the grains are strongly seriticized and some contain minor perthite exsolutions. Quartz is anhedral and shows undulatory extinction. Plagioclase is usually euhedral, and seriticized. Biotite flakes are 0.1 to 1 mm in size, and alteration to chlorite is common. Zircon and apatite are common accessory phases.

In Tuuliniemi, red and gray varieties of the vein granite are observed. The red fine- to medium-grained granite is leucocratic with minor biotite as the mafic phase. Feldspars are strongly altered, especially potassium feldspar, which is the dominant phase. Potassium feldspar crystals are anhedral to euhedral and 0.5 to 2 mm in size. Plagioclase is euhedral, and 1 to 3 mm in size. Quartz is anhedral and shows weak undulatory extinction and ranges from 0.2 to 2 mm. Biotite flakes are completely chloritized. Common accessory minerals are titanite, zircon, and fluorite. Some epidote is observed as an alteration product of plagioclase. The grey granite is fine- and even-grained, and granophyric texture is common. The anhedral potassium feldspar crystals are unaltered, and about 0.5–1 mm in grain size. Minor small plagioclase crystals (<0.5 mm) are euhedral and strongly altered. Compared to the red granite biotite is more abundant, unaltered, and its grain size varies from 0.1 to ~1 mm.

## 5.3. Hybrid rocks

The hybrid rocks show porphyritic texture due to large (1–2 cm) potassium feldspar xenocrysts. The groundmass is in many ways mineralogically

similar to the monzodioritic rocks. Potassium feldspar is also present in the groundmass with interstitial quartz (Fig. 5f). Plagioclase is euhedral and partially skeletal, and the grain size ranges from 0.5 to 5 mm. Twinning is common and some grains are sericitisized. Hornblende is poikilitic, shows dark green-brown pleochroism and occurs together with biotite. A notable observation is that whereas pyroxenes are ubiquitous in all of the monzodioritic rock types they are completely absent in the hybrid rocks.

### 5.4. Contacts between the monzodioritic pillows and granitic veins

The contacts between the monzodioritic pillows and granitic veins are irregular and somewhat gradational in Pärnäjärvi. In Tuuliniemi the contacts are seemingly sharper but their microscopic and mineralogical features are broadly similar in both areas. In the pillows, biotite and amphibole form a zoned rim at the contact (Fig. 5g & h): outer pillow contact zone is dominated by biotite phenocrysts and the inner zone includes both biotite and amphibole phenocrysts. In the granites there is a very thin and fine-grained rim at the contact. Myrmekite and granophyric textures are particularly common near the contact. Apophyses from the interstitial granite to the monzodioritic pillows are common, and their contacts against monzodiorite are always sharp (Fig. 5h).

## 6. Geochemistry

The following section summarizes key geochemical features of the XRF data presented in Figures 6 and 7 and in Table 2.

### 6.1. Mafic rocks

The mafic rocks show variable silica contents (45–53 wt.%) and the olivine monzodiorites are the most mafic samples**.** The rest of the monzodioritic rocks have rather consistent silica content, but they show more variation in other major element compositions (Fig. 6). The monzodioritic rocks exhibit negative trends in $FeO^{tot}$, MnO, MgO, and CaO with increasing silica content. The olivine monzodiorites are the most primitive mafic rocks with Mg-number of 40–49. Pillows from Pärnäjärvi and Tuuliniemi have Mg# of 41–42 and 33–36, respectively, and the massive monzodiorites are the most evolved with Mg# of 26–28 (Table 2).

The monzodioritic pillows from the different study areas have broadly similar major element compositions but some regional differences are observed. The pillows in Tuuliniemi are usually relatively higher in $TiO_2$ (2.7–2.8 wt.%). $P_2O_5$ (0.89–0.94 wt.%), and $K_2O$ (1.2–2.3 wt.%) compared to Pärnäjärvi ($TiO_2$ 2.5–2.6 wt.%, $P_2O_5$ 0.74–0.76, and $K_2O$ 1.2–1.4 wt.%). In contrast, the pillows in Pärnäjärvi have higher MgO (4.6–5 wt.%), $FeO^{tot}$ (13.7–14.4 wt.%) and CaO (6.2–6.6 wt.%) than those of Tuuliniemi (MgO 3–3.5 wt.%, $FeO^{tot}$ 12.9–13.9 wt.%, and CaO 5.9–6.2 wt.%, Fig. 6, Table 2). The massive monzodiorites have higher $K_2O$ (3.3–3.6 wt.%), $P_2O_5$ (1.05–1.07 wt.%), and $FeO^{tot}$ (14.2–14.6 wt.%), and are lower in MgO (2.4–2.6 wt.%) and $Al_2O_3$ (13.2–13.3 wt.%) than the pillows. The pillow rims are lower in CaO (4.2–5.4 wt.%) and $Na_2O$ (2–2.2 wt.%) compared to the pillow centers (2.6–3.1 wt.%). When comparing the pillow rim samples of Tuuliniemi and Pärnäjärvi, the sample from Tuuliniemi has higher $FeO^{tot}$ (15.1 wt.%) and MnO (0.21 wt.%) than in Pärnäjärvi ($FeO^{tot}$ 13.6, MnO 0.18 wt.%), and the sample from Pärnäjärvi has higher $K_2O$ (3.3 wt.%) than in Tuuliniemi (1.5 wt.%).

The anorthositic rocks have similar silica contents but lower $TiO_2$ (1–1.3 wt.%), $FeO^{tot}$ (5.4–7.3 wt.%), MnO (0.07–0.1 wt.%), MgO (1.4–1.9 wt.%), and $P_2O_5$ (0.3–0.4 wt.%), and higher $Al_2O_3$ (21–23 wt.%), CaO (8.3–8.5 wt.%), and $Na_2O$ (3.6–3.9 wt.%) than the other mafic rocks as a result of plagioclase accumulation (Fig. 6). The anorthositic rocks have similar Mg# 35–36 as the pillows in Tuuliniemi.

Table 2. Whole-rock XRF data of the 33 samples from the Ahvenisto complex as major element oxide compositions and selected trace elements in ppm.

| Sample | APHE-14-011.5.X2 | APHE-14-011.E.X1 | RMF-15-101-A.X1 | APHE-14-012.1.X1 | APHE-14-013.1.X1 | APHE-14-013.1.X4 | APHE-14-013.B.X1 | RMF-15-126-A.X2 | APHE-14-011.F.X1 | APHE-14-013.1.X3 |
|---|---|---|---|---|---|---|---|---|---|---|
| Rock type | Pillow | Pillow | Pillow | Pillow | Pillow | Pillow | Pillow | Pillow | Pillow rim | Pillow rim |
| Area | Pärnäjärvi | Pärnäjärvi | Pärnäjärvi | Tuuliniemi | Tuuliniemi | Tuuliniemi | Tuuliniemi | Tuuliniemi | Pärnäjärvi | Tuuliniemi |
| Major elements (wt.-%) | | | | | | | | | | |
| $SiO_2$ | 51.38 | 50.69 | 51.28 | 53.06 | 52.47 | 51.76 | 51.85 | 52.54 | 51.16 | 51.63 |
| $TiO_2$ | 2.46 | 2.55 | 2.46 | 2.65 | 2.78 | 2.81 | 2.79 | 2.76 | 2.5 | 2.82 |
| $Al_2O_3$ | 14.38 | 14.29 | 14.95 | 14.22 | 14.3 | 14.22 | 14.13 | 14.62 | 14.45 | 13.94 |
| FeO | 13.93 | 14.44 | 13.7 | 13.06 | 13.5 | 13.86 | 13.77 | 12.91 | 13.56 | 15.13 |
| MnO | 0.18 | 0.19 | 0.18 | 0.16 | 0.17 | 0.18 | 0.18 | 0.19 | 0.18 | 0.21 |
| MgO | 4.87 | 5.03 | 4.57 | 3.05 | 3.29 | 3.44 | 3.35 | 3.47 | 4.69 | 3.66 |
| CaO | 6.24 | 6.53 | 6.61 | 5.88 | 6.17 | 6.19 | 6.14 | 6.02 | 5.37 | 4.19 |
| $Na_2O$ | 2.66 | 2.63 | 2.78 | 2.51 | 2.93 | 2.73 | 2.7 | 3.14 | 1.99 | 2.22 |
| $K_2O$ | 1.22 | 1.4 | 1.2 | 2.11 | 1.53 | 2.33 | 2.27 | 1.16 | 3.27 | 1.52 |
| $P_2O_5$ | 0.74 | 0.76 | 0.74 | 0.89 | 0.93 | 0.93 | 0.94 | 0.9 | 0.75 | 0.94 |
| Sum | 98.05 | 98.52 | 98.48 | 97.59 | 98.09 | 98.45 | 98.11 | 97.7 | 97.93 | 96.25 |
| Trace elements (ppm) | | | | | | | | | | |
| Ba | 744 | 863 | 748 | 1032 | 1012 | 1020 | 1028 | 884 | 349 | 396 |
| Cu | 40 | 42 | 38 | 45 | 42 | 34 | 39 | 59 | 43 | 47 |
| Cr | 24 | 24 | 31 | 16 | 19 | 16 | 15 | 28 | 37 | 16 |
| Ni | 34 | 37 | 30 | 11 | 15 | 14 | 17 | 13 | 35 | 12 |
| Sr | 332 | 372 | 363 | 330 | 342 | 347 | 335 | 346 | 258 | 208 |
| Zn | 179 | 183 | 180 | 200 | 181 | 204 | 191 | 159 | 198 | 251 |
| Zr | 287 | 316 | 292 | 402 | 386 | 372 | 400 | 392 | 262 | 328 |
| Rb | 88 | 90 | 67 | 96 | 74 | 87 | 90 | 70 | 379 | 133 |
| Nb | 22 | 23 | 22 | 29 | 28 | 28 | 27 | 27 | 24 | 41 |
| Y | 60 | 53 | 57 | 63 | 70 | 65 | 74 | 68 | 57 | 90 |
| Ce | 97 | 117 | 76 | 130 | 127 | 119 | 75 | 132 | 109 | 128 |
| La | 41 | 34 | 54 | 63 | 58 | 41 | 51 | 52 | 24 | 44 |
| V | 127 | 136 | 135 | 139 | 136 | 140 | 140 | 147 | 136 | 135 |
| U | 5 | <2 | 3 | 5 | 6 | 6 | 8 | 5 | 4 | 5 |

Table 2 continued...

| RMF-15-112-A.X1 | RMF-15-116-A.X1 | APHE-16-5-A | APHE-16-6-A | RMF-15-122-A.X1 | APHE-16-11-A | RMF-15-106-A.X1 | RMF-15-106-A.X1.2 | RMF-15-111-A | RMF-15-115-A.X1 | RMF-15-115-C.X1 |
|---|---|---|---|---|---|---|---|---|---|---|
| Monzodiorite | Monzodiorite | Ol-monzodiorite | Ol-monzodiorite | Ol-monzodiorite | Ol-monzodiorite | Anorthositic | Anorthositic | Hybrid | Hybrid | Hybrid |
| Pärnäjärvi | Pärnäjärvi | Iso Kuoppalampi | Iso Kuoppalampi | Iso Kuoppalampi | Iso Kuoppalampi | Pärnäjärvi | Pärnäjärvi | Pärnäjärvi | Pärnäjärvi | Pärnäjärvi |
| 52.09 | 53.23 | 49.16 | 47.9 | 49.47 | 45.42 | 53.05 | 53.02 | 57.16 | 56.08 | 56.52 |
| 2.65 | 2.55 | 3 | 1.57 | 2.38 | 2.23 | 1.26 | 0.99 | 1.95 | 2.08 | 2 |
| 13.28 | 13.2 | 14.62 | 14.26 | 13.85 | 17.98 | 21.05 | 23.01 | 13.39 | 12.63 | 13.68 |
| 14.61 | 14.15 | 15.24 | 16.17 | 15.68 | 12.19 | 7.29 | 5.41 | 11.87 | 12.09 | 11.83 |
| 0.2 | 0.2 | 0.2 | 0.19 | 0.21 | 0.14 | 0.1 | 0.07 | 0.16 | 0.16 | 0.17 |
| 2.64 | 2.44 | 4.77 | 8.94 | 6.92 | 5.59 | 1.92 | 1.42 | 1.84 | 1.77 | 1.94 |
| 5.95 | 5.91 | 7 | 6.03 | 6.44 | 7.14 | 8.25 | 8.51 | 5.08 | 5.15 | 4.54 |
| 2.67 | 2.59 | 2.52 | 2.4 | 2.45 | 2.92 | 3.63 | 3.86 | 2.69 | 2.25 | 2.94 |
| 3.31 | 3.61 | 1.56 | 1.42 | 1.57 | 2.32 | 1.62 | 1.73 | 3.61 | 4.56 | 3.11 |
| 1.05 | 1.07 | 0.92 | 0.47 | 0.61 | 0.82 | 0.43 | 0.31 | 0.86 | 0.91 | 0.73 |
| 98.43 | 98.93 | 98.98 | 99.35 | 99.58 | 96.75 | 98.59 | 98.33 | 98.61 | 97.68 | 97.45 |
| 1262 | 1179 | 734 | 589 | 652 | 316 | 600 | 682 | 1006 | 1396 | 1198 |
| 37 | 44 | 38 | 25 | 39 | 28 | 29 | 21 | 32 | 23 | 28 |
| <5 | <5 | 34 | 15 | 54 | 8 | 12 | <5 | <5 | <5 | <5 |
| 7 | 5 | 28 | 93 | 58 | 16 | 8 | <2 | <2 | <2 | 2 |
| 278 | 292 | 366 | 368 | 379 | 646 | 629 | 665 | 239 | 204 | 262 |
| 248 | 230 | 183 | 177 | 183 | 131 | 114 | 79 | 222 | 176 | 205 |
| 414 | 217 | 244 | 206 | 247 | 59 | 157 | 159 | 511 | 932 | 470 |
| 81 | 111 | 51 | 41 | 48 | 223 | 64 | 65 | 110 | 125 | 96 |
| 36 | 36 | 24 | 16 | 21 | 15 | 14 | 11 | 38 | 33 | 38 |
| 85 | 86 | 61 | 46 | 42 | 55 | 34 | 28 | 90 | 101 | 88 |
| 143 | 175 | 93 | 67 | 86 | 75 | 67 | 59 | 148 | 197 | 111 |
| 67 | 74 | 38 | 21 | 34 | 22 | 26 | 16 | 78 | 84 | 70 |
| 73 | 80 | 162 | 87 | 139 | 285 | 93 | 56 | 44 | 52 | 49 |
| 4 | 2 | 4 | 4 | <2 | 2 | <2 | 2 | 6 | 6 | 6 |

Table 2 continued...

| APHE-14-011.3.X1 | APHE-14-011.5.X1 | APHE-14-011.F.X2 | APHE-14-013.1.X2 | APHE-14-013.1.X5 | RMF-15-126-A.X1 | RMF-15-125-A.X1 | RMF-15-128-A.X1 | RMF-15-136-A.X1 | RMF-15-114-A.X1 | RMF-15-115-A.X2 | RMF-15-115-B.X1 |
|---|---|---|---|---|---|---|---|---|---|---|---|
| Vein granite | Vein granite | Vein granite | Vein granite | Vein granite | Vein granite | Leucogranite | Leucogranite | Leucogranite | Hbl-granite | Hbl-granite | Hbl-granite |
| Pärnäjärvi | Pärnäjärvi | Pärnäjärvi | Tuuliniemi | Tuuliniemi | Tuuliniemi | Tuuliniemi | Tuuliniemi | Tuuliniemi | Pärnäjärvi | Pärnäjärvi | Pärnäjärvi |
| 72.19 | 72.58 | 72.24 | 72.14 | 69.7 | 74.59 | 75.67 | 72.14 | 73.66 | 68.24 | 68.55 | 68.33 |
| 0.28 | 0.29 | 0.3 | 0.28 | 0.64 | 0.22 | 0.1 | 0.35 | 0.33 | 0.61 | 0.79 | 0.62 |
| 13.63 | 13.72 | 13.77 | 13.12 | 13.65 | 13.2 | 13.91 | 13.77 | 13.3 | 13.15 | 13.22 | 13.39 |
| 1.99 | 1.91 | 2.14 | 2.38 | 4.13 | 1.59 | 1.01 | 2.32 | 2.3 | 6.04 | 6.57 | 5.32 |
| 0.03 | 0.03 | 0.03 | 0.03 | 0.05 | 0.03 | 0.02 | 0.03 | 0.03 | 0.1 | 0.08 | 0.07 |
| 0.44 | 0.4 | 0.42 | 0.48 | 0.73 | 0.3 | 0.15 | 0.4 | 0.28 | 0.18 | 0.38 | 0.21 |
| 0.85 | 0.87 | 0.94 | 0.45 | 1.54 | 0.3 | 1.08 | 0.68 | 0.66 | 2.25 | 1.86 | 1.83 |
| 2.74 | 2.74 | 2.77 | 1.71 | 2.24 | 2.56 | 3.59 | 2.63 | 2.58 | 2.93 | 3.12 | 2.82 |
| 6.49 | 6.55 | 6.52 | 8 | 6 | 6.84 | 4.2 | 6.34 | 6.39 | 5.73 | 4.04 | 5.91 |
| 0.18 | 0.17 | 0.19 | 0.14 | 0.26 | 0.11 | 0.09 | 0.1 | 0.12 | 0.08 | 0.13 | 0.08 |
| 98.84 | 99.25 | 99.33 | 98.71 | 98.93 | 99.72 | 99.83 | 98.76 | 99.66 | 99.31 | 98.73 | 98.58 |
| 449 | 472 | 458 | 864 | 710 | 570 | 534 | 361 | 392 | 1338 | 1016 | 1340 |
| 9 | 12 | 9 | 7 | 12 | 9 | 5 | 13 | 12 | 19 | 21 | 15 |
| <5 | <5 | <5 | <5 | <5 | <5 | <5 | <5 | <5 | <5 | <5 | <5 |
| <2 | <2 | <2 | <2 | <2 | <2 | <2 | <2 | <2 | <2 | <2 | <2 |
| 68 | 68 | 69 | 52 | 146 | 124 | 292 | 76 | 63 | 110 | 169 | 104 |
| 28 | 36 | 39 | 22 | 87 | 15 | 25 | 40 | 47 | 179 | 93 | 160 |
| 170 | 157 | 162 | 173 | 279 | 140 | 96 | 195 | 255 | 807 | 1403 | 859 |
| 355 | 350 | 369 | 284 | 280 | 273 | 199 | 330 | 400 | 183 | 125 | 182 |
| 19 | 17 | 19 | 12 | 22 | 13 | 10 | 19 | 22 | 49 | 13 | 55 |
| 25 | 33 | 28 | 47 | 43 | 11 | 24 | 30 | 49 | 89 | 47 | 67 |
| 60 | 62 | 110 | 142 | 97 | 85 | 77 | 140 | 130 | 194 | 111 | 140 |
| 30 | 42 | 41 | 56 | 49 | 45 | 25 | 69 | 68 | 97 | 56 | 58 |
| 11 | 9 | 7 | 11 | 11 | 7 | 8 | 8 | <4 | <4 | <4 | <4 |
| 12 | 10 | 13 | 10 | 7 | 7 | 5 | 15 | 9 | 4 | 5 | 9 |

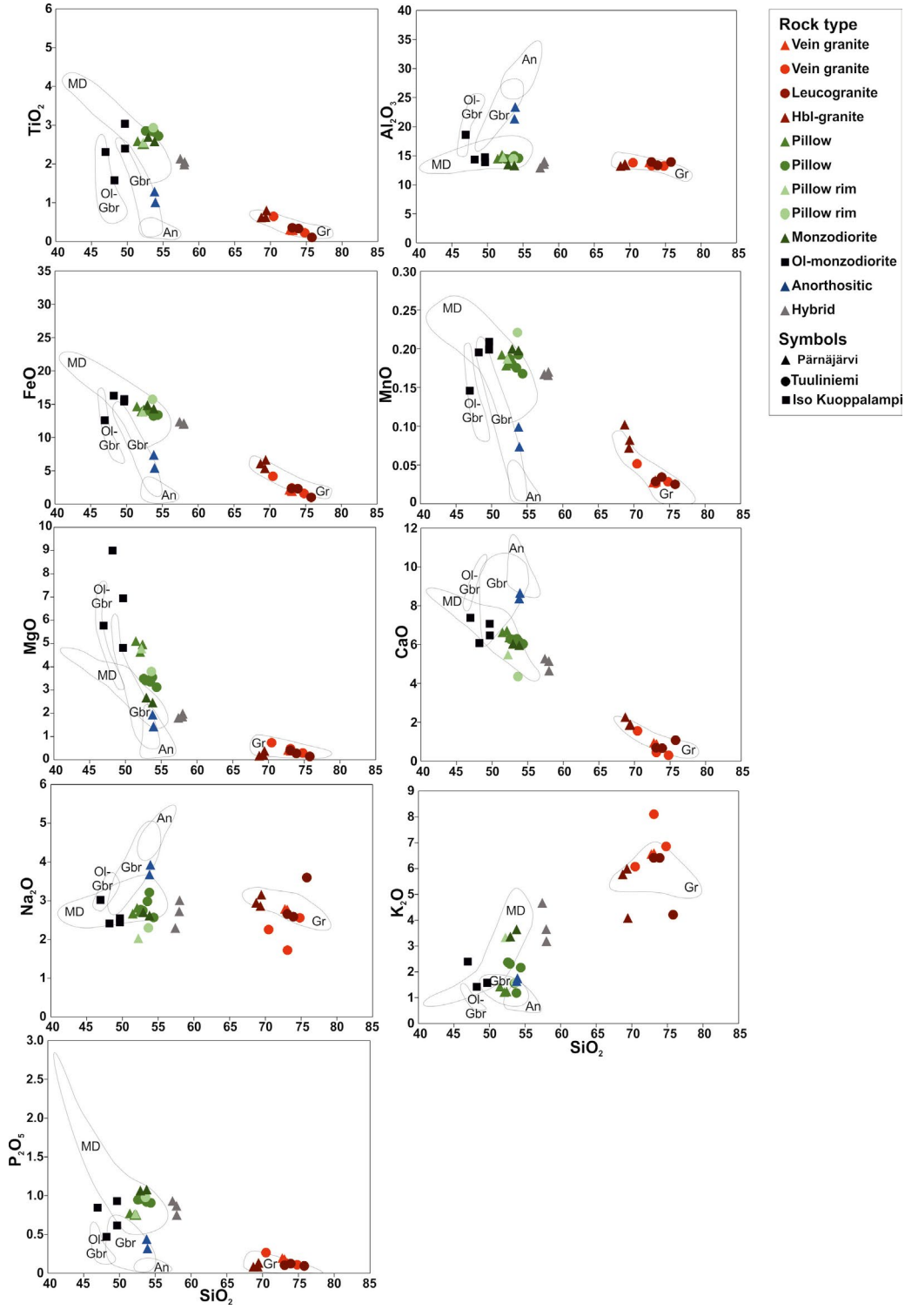


Figure 6. $SiO_2$ (wt.%) vs. major element oxide (wt.%) diagrams showing geochemical features of the different rock types from Ahvenisto. Areas of earlier analyses from Johanson (1984) and Heinonen et al (2010b) are marked with dotted lines.

Most of the trace element compositions in the monzodioritic rocks display positive correlation with $SiO_2$, except for Sr that has a negative correlation most likely due to plagioclase fractionation. However, one olivine monzodiorite sample has high Rb and Sr and low Ba contents that may reflect strong feldspar accumulation. The pillow rims show relative enrichment in Rb and depletion in Ba relative to the pillow centers which may result from stronger effect of chemical exchange closer to the granite contact (Fig. 7).

## 6.2. Granites

The granitic rocks show variation in their silica content with $SiO_2$ 68.2–75.7 wt.%. The vein granites have $SiO_2$ of 69.7–74.6 wt.% in Tuuliniemi and 72.2–72.6 wt.% in Pärnäjärvi (Table 2). The granites show negative correlation in $TiO_2$, $FeO^{tot}$, MnO, and CaO with silica. Granites have similar $Al_2O_3$ (13.2–13.9 wt.%) and MgO (0.2–0.7 wt.%), but wide ranges in $Na_2O$ (1.7–3.6 wt.%) and $K_2O$ (4–8 wt.%; Fig. 6). The hbl-granites represent the most primitive members of the granitic series with lowest silica content, but they have a higher Fe/Mg ratio than the other granites of the complex (Fig. 6, Table 2). Trace element compositions of the granites usually display negative correlation with increasing silica content, except for Rb the trend being positive due to potassium feldspar accumulation (Fig. 7). Trace element compositions of the granites show more variation than in the other rock types. The granites are metaluminous to peraluminous, and they display general ferroan (A-type) geochemical characteristics broadly concurrent with analyses from previous studies (Johanson, 1984; Alviola et al., 1999; Heinonen et al., 2010b).

## 6.3. Hybrid rocks

The hybrid rock samples have a rather homogeneous major element composition in $SiO_2$, $TiO_2$, $Al_2O_3$, $FeO^{tot}$, MnO, MgO,and CaO, but show some variation in $Na_2O$, $K_2O$, and $P_2O_5$ (Fig. 6, Table 2). The hybrid rocks plot onto a trend from granites to monzodioritic rocks in $SiO_2$, $TiO_2$, $FeO^{tot}$, MnO, CaO, and MgO variation diagrams. The hybrid rock samples exhibit also homogeneous trace element composition, with minute variation in Ba, Zn, Ce, and Zr. High Zr content of one hybrid sample (RMF-15-115.A.X1) most likely represents zircon derived from hbl-granite (Fig. 7). Similar trends observed for major elements are found also for many trace elements as the hybrid rocks plot between hbl-granite and monzodioritic compositions. Judging from these geochemical results the massive monzodiorite seems to be the most likely candidate for the mafic end-member composition in a possible mixing scenario discussed in section 7.3 below.

# 7. Discussion

## 7.1. Magmatic evolution of the monzodioritic rocks

The compositional trends defined by the different monzodioritic rock types (olivine monzodiorite to pillows to massive monzodiorite) can be interpreted as an evolution trend of a mafic magma (Fig. 8). In this interpretation the olivine monzodiorites (Mg# 40–49) could represent the most primitive or a parental composition to a monzodioritic fractionation trend. The pillows from both study areas would represent their own intermediate stages, Pärnäjärvi a slightly less (Mg# 41–42) and Tuuliniemi (Mg# 33–36) somewhat more evolved, and the massive monzodiorites (Mg# 27–28) the most evolved compositions. Assuming that the monzodioritic rocks represent compositions of magmatic liquids at different stages of the potential mafic fractionation, a more detailed geochemical consideration of magma interaction styles in the Ahvenisto complex is enabled.

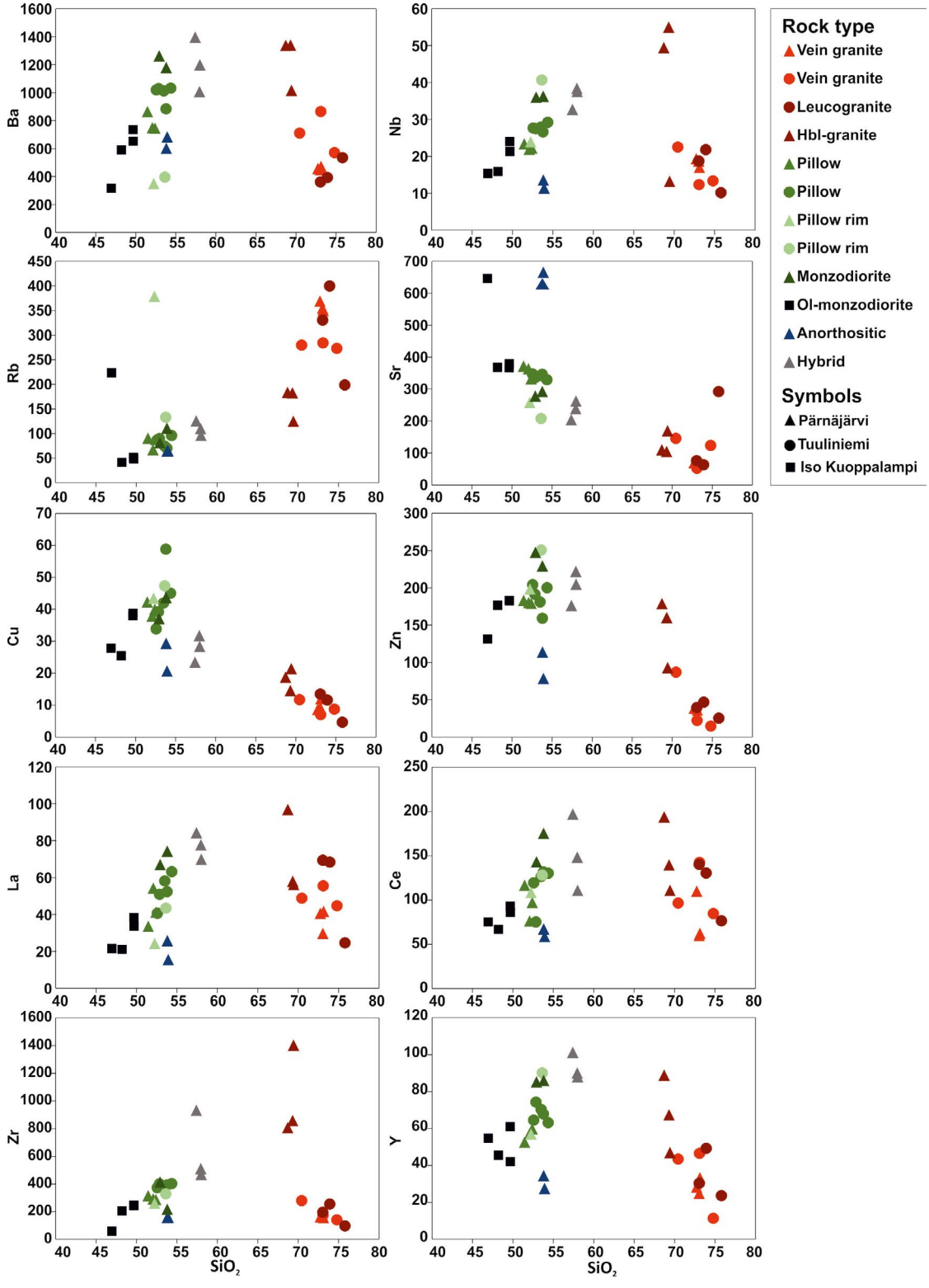


Figure 7. $SiO_2$ (wt.%) vs. trace element (ppm) diagrams of selected elements, showing indistinct but consistent trends in chemical evolution between the different sample types from Ahvenisto

## 7.2. Petrographical and geochemical constraints on mixing and mingling

As reported earlier (Johanson, 1984; Alviola et al., 1999) field relations reveal that both mingling and mixing play important roles in forming the net-veined pillow structures and hybrid rocks in the Ahvenisto complex. Similar field relations to those at Ahvenisto complex have been found from other mingling locations, like in the Jaala-Iitti complex, Finland (Salonsaari, 1995), Newark Island layered intrusion (Wiebe, 1993) and Austurhorn, Iceland (Blake et al., 1965; Weidendorfer et al., 2014; Padilla et al., 2016). The following processes that have been suggested in other studies also apply to the Ahvenisto complex. The rims in the pillows, as well as their diffusive contacts, indicate exchange of components between the granite and the pillows. Clusters of plagioclase laths imply rapid crystallization of the pillows. The granite apophyses crosscutting pillows suggest that at the time the pillow magmas had already crystallized the granitic material has still been at least partially liquid (Blake et al., 1965; Wiebe, 1993; Weidendorfer et al., 2014; Padilla et al., 2016). These interpretations are also supported by petrographic observations: the pillows show an amphibole-biotite rim next to the contact with the granitic veins indicating exchange of $H_2O$ and other components from the granite to the pillows (Wiebe et al., 2001). Near the contacts of the pillows, pyroxene phenocrysts are replaced by secondary amphibole, but in the pillow center, pyroxenes also occur as unaltered crystals. This feature was also observed in the pillows at Vinalhaven, Maine and Austurhorn intrusions, Iceland (Wiebe et al., 2001; Weidendorfer et al., 2014).

The mingling structures seem to be the dominant feature in all three study areas at Ahvenisto complex. Hybridization is a more local phenomenon and not observed in the northernmost Tuuliniemi -study area. The olivine monzodiorite is only observed at Iso Kuoppalampi area in the south. These differences between northern and southern parts of the Ahvenisto complex might arise from different level of erosion. Where the contact between monzodiorite and hbl-granite is visible, it is observed that the hbl-granite intrudes between the monzodioritic pillows as veins, indicating that the net-veined granite originates from the hbl-granite. The vein granites, however, have finer grain size and are more leucocratic than the hbl-granite possibly resulting from the proximity of the mafic magma that superheated the hbl-granite magma. Near the contact of the hbl-granite and the monzodioritic rocks at Pärnäjärvi area, mingling structures, hybridization, and massive monzodiorite are observed together with complex relationships. In addition, the unclear contacts with the country rocks in Tuuliniemi area reflect the complex origin of these structures. The leucocratic granite sheet observed in Tuuliniemi might represent the same granitic melt that was formed by superheating of the hbl-granitic magma.

In the pillows, potassium feldspar is absent or occurs only as a minor mineral suggesting that the pillows are ferrodiorites rather than monzodiorites. In massive monzodiorite, potassium feldspar occurs with plagioclase and quartz, and amphibole and pyroxene are the mafic phases. The more mafic olivine monzodiorite in the Iso Kuoppalampi area also contains potassium feldspar, but with olivine and pyroxenes as the mafic phases. The mineral composition of the hybrid rock (plagioclase, quartz, potassium feldspar, amphibole, biotite, minor olivine, and potassium feldspar phenocrysts) suggest that some degree of chemical mixing took place in addition to transport of potassium feldspar phenocrysts into the monzodioritic melt from the granitic melt. Chemical mixing of magmas produced a new unique homogenous liquid phase.

Geochemical evidence corroborates the observations made from field relations and petrography: the pillows and olivine monzodiorite show lower K and Rb, higher Mg content, and slightly higher Al, Ca, and Sr contents than the massive monzodiorite due to the proportions of feldspars and Mg/Fe-silicates. The different monzodiorite types follow a decreasing Mg#

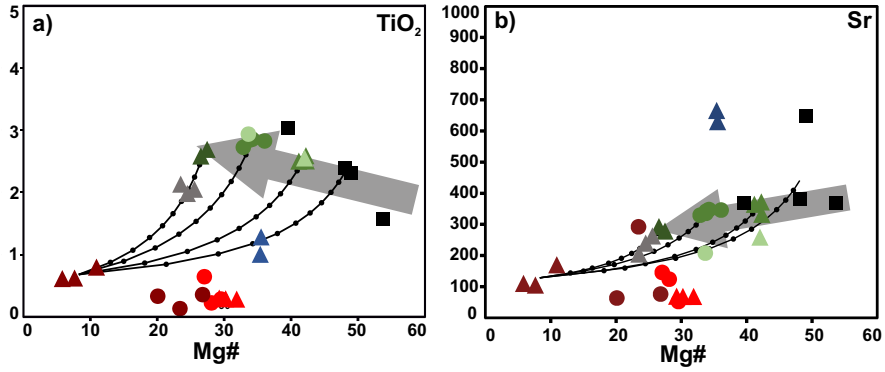


Figure 8. Illustration of the inferred compositional evolution and chemical mixing of the monzodioritic magmas in (a) Mg# vs. TiO2 (wt.%) and (b) Mg# vs. Sr (ppm) diagrams. The suggested approximate fractionation trend for the monzodioritic rocks is denoted by a gray arrow and mixing trends calculated between different monzodioritic compositions (ol-monzodiorite, massive monzodiorite, pillows from Pärnäjärvi and Tuuliniemi) and an average hbl-granite are shown by black solid lines with 10 % intervals.

trend from olivine monzodiorite to the massive monzodiorite, which is suggested to conform to a fractionation trend (Fig. 8). Compared to the monzodioritic rocks, the hybrid rocks plot on a diverging compositional trend, which is interpreted as mixing trend rather than liquid line of descent of the mafic magma. In general, our geochemical results are consistent with the previous analyses from the Ahvenisto complex (Johanson, 1984; Heinonen et al., 2010b) and fit the suggested fractionation trend of the Ahvenisto rocks (Heinonen et al., 2010b).

## 7.3. Modeling of mixing and mingling

Field observations, mineral composition, and geochemical composition of the studied Ahvenisto samples suggest that chemical mixing between mafic and felsic magmas has occurred and produced a hybrid melt. For two different magmas to be able to mix they must have similar ranges in viscosity and temperature (Sparks & Marshall, 1986).

The chemical and physical feasibility of mixing of felsic and mafic magmas in the Ahvenisto complex was evaluated using the hbl-granite as the felsic end-member and different monzodioritic compositions as mafic end-members. In Figure 8, the calculated mixing lines are plotted in $TiO_2$ and La vs. Mg# [$Mg^{2+}/(Mg^{2+}+Fe^{2+})$] diagrams. The mixing lines were calculated using the average composition of hbl-granite mixed with the average compositions of 1) massive monzodiorite, 2) monzodiorite pillows from the two study areas, and 3) olivine monzodiorite using the equation:

$$X_H^i - X_F^i = M_m(X_M^i - X_F^i) \quad (4)$$

where $X_F^i$ is the concentration of element $i$ in felsic end-member, $X_M^i$ in mafic end-member, and $X_H^i$ in hybrid (Fourcade & Allegre, 1981). $M_m$ is the weight proportion of mafic magma, and mixtures were calculated in 10% intervals from 10 to 90 percent.

The mixing trends suggest that the massive monzodiorite most likely represents the mafic end-member of the hybrid rocks when the felsic end-member is presumed to be similar to the average composition of the hbl-granite. The mass fraction of the mafic magma in the mixture ($X_m$) has been evaluated using the least sum of squares method in Figure 9, where $X_H$-$X_F$ versus $X_M$-$X_F$ are plotted for i = $SiO_2$, MnO, $TiO_2$, MgO, CaO, and FeO (cf. Salonsaari, 1995). The hybrid rocks seem to have formed by mixing of the two end-members with a relatively high mafic mass fraction $X_m$ = 0.71–0.75, i.e. mafic-felsic proportions of ca. 3:1.

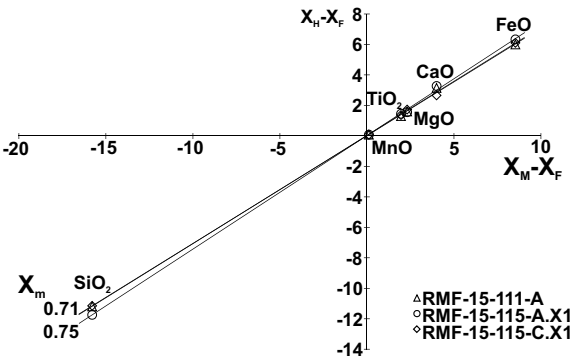


Figure 9. Illustration of the least sum of squares mixing test that was used to evaluate the relative proportions of mafic and felsic magmas involved in the mixing process in the hybrid rocks from Ahvenisto. The model implies that the mafic/felsic-ratio was ca. 3:1.

According to Sparks and Marshall (1986), the viscosities of two adjacent magmas at thermal equilibrium control, whether mixing is possible. They also argue that mixing can be selective (some compositions do no readily mix), and that the proportions and compositions of the interacting magmas regulate the process so that a hybrid magma can contain large proportion of felsic material only when the mafic component represents a relatively evolved composition. Our mixing models are compatible with these arguments, thus only the most evolved mafic magmas seems to have mixed with the felsic material. Also, the calculated viscosity difference of these two magmas is smaller (near thermal equilibrium, Fig. 10) than it is between either the pillow material or olivine monzodiorite as dry melts.

A melt viscosity model (Giordano et al., 2008) based on whole-rock geochemical composition was used to estimate the melt viscosities of the samples. In the model, the non-Arrhenian temperature dependence of viscosity is modeled by the VFT (Vogel-Fulcher-Tamman) equation:

$$\log \eta = A + \frac{B}{T(K) - C} \quad (1)$$

where A is a constant parameter, and parameters B and C depend on the major element and volatile compositions of the melt. Parameters B and C contain 17 geochemical coefficients and can be calculated from the following equations:

$$B = \sum_{i=1}^{7} [b_i M_i] + \sum_{j=1}^{3} [b_{1j}(M1_{1j} M2_{1j})] \quad (2)$$

$$C = \sum_{i=1}^{6} [c_i N_i] + [c_{11}(N1_{11} N2_{11})] \quad (3)$$

where M and N are the coefficients for combinations of mol. % oxides (b and c).

The melt viscosities for dry melts and melts with 1 wt.% and 2.5 wt.% of $H_2O$ at different temperatures were determined together with liquidus temperatures (Table 3, Electronic Appendix D) using Pele software (Boudreau, 1999), for the chosen whole-rock compositions. Liquidus temperatures were calculated starting at 4 kbar and QFM buffer and the crystallizing phases were restricted to those observed in the rocks: plagioclase, quartz, alkali feldspar, pyroxene, amphibole, biotite, olivine, magnetite, and ilmenite. The effects of magma solidosities were considered minute and omitted for simplicity.

Field relations of the mingling structures (Fig. 10c) reveal that both magmas behaved as liquids at the same time, and that the pillow-forming mafic magma was more viscous than the vein-forming felsic magma ($\log \eta_{gr} < \log \eta_{md}$). However, the viscosity calculations show that at liquidus temperatures in dry melts $\log \eta_{gr} > \log \eta_{md}$. This suggests that the proportion of mafic magma may have been large enough to heat the felsic magma to lower its viscosity. At the same time the mafic magma cooled down and got more viscous. With only a small amount of heat loss from the mafic magma and elevated temperature of the felsic magma, the viscosity values of the magmas can be reversed, so that $\log \eta_{gr} < \log \eta_{md}$. $\log \eta_{gr} \approx \log \eta_{md}$ when $T_{gr}$ would be 1070 °C and $T_{md}$ at 1130 °C (Fig. 10a). However, this discrepancy can also be accounted for by considering the different volatile compositions of the magmas.

Table 3. Average melt viscosities calculated for the Ahvenisto rock types using the equations of Giordano et al. (2008) at different temperatures and volatile compositions. Liquidus temperatures were determined using Pele software (Boudreau, 1999).

| | Vein granite | Leucogranite | Hbl-granite | Pillow | Pillow rim | Monzodiorite | Ol-monzodiorite | Anorthositic | Hybrid |
|---|---|---|---|---|---|---|---|---|---|
| T(°C) | Viscosities with 2.5 w.-% H2O | | | | | | | | |
| 1500 | 1.6 | 1.6 | 1.5 | 1.5 | 1.6 | 1.4 | 1.4 | 0.8 | 1.4 |
| 1400 | 2.0 | 2.0 | 1.9 | 2.0 | 2.1 | 1.9 | 1.9 | 1.2 | 1.9 |
| 1300 | 2.4 | 2.4 | 2.4 | 2.5 | 2.7 | 2.4 | 2.5 | 1.7 | 2.4 |
| 1200 | 2.9 | 2.9 | 2.9 | 3.1 | 3.3 | 3.0 | 3.2 | 2.2 | 3.0 |
| 1100 | 3.5 | 3.5 | 3.5 | 3.9 | 4.1 | 3.7 | 4.0 | 2.9 | 3.7 |
| 1000 | 4.2 | 4.2 | 4.3 | 4.8 | 5.1 | 4.6 | 5.0 | 3.8 | 4.5 |
| 900 | 5.0 | 5.0 | 5.1 | 6.0 | 6.3 | 5.7 | 6.2 | 4.8 | 5.6 |
| 800 | 6.0 | 6.0 | 6.2 | 7.5 | 7.8 | 7.2 | 7.9 | 6.1 | 6.9 |
| 700 | 7.2 | 7.3 | 7.5 | 9.6 | 9.8 | 9.0 | 10.2 | 7.9 | 8.6 |
| 600 | 8.8 | 8.8 | 9.2 | 12.4 | 12.7 | 11.6 | 13.5 | 10.4 | 10.9 |
| $T_l$(°C) | 936.5 | 908.1 | 965.1 | 1138.1 | 1170.4 | 1120.4 | 1214.7 | 1127.1 | 1099.4 |
| | Viscosities with 1 w.-% H2O | | | | | | | | |
| 1500 | 2.4 | 2.4 | 2.3 | 2.2 | 2.4 | 2.1 | 2.1 | 1.5 | 2.2 |
| 1400 | 2.8 | 2.8 | 2.8 | 2.7 | 2.9 | 2.6 | 2.7 | 1.9 | 2.7 |
| 1300 | 3.3 | 3.4 | 3.3 | 3.4 | 3.6 | 3.3 | 3.3 | 2.5 | 3.3 |
| 1200 | 4.0 | 4.0 | 4.0 | 4.1 | 4.3 | 4.0 | 4.1 | 3.2 | 4.0 |
| 1100 | 4.7 | 4.7 | 4.7 | 5.1 | 5.3 | 4.9 | 5.1 | 4.0 | 4.8 |
| 1000 | 5.5 | 5.5 | 5.6 | 6.2 | 6.5 | 6.0 | 6.3 | 5.0 | 5.9 |
| 900 | 6.5 | 6.6 | 6.7 | 7.7 | 7.9 | 7.3 | 7.8 | 6.3 | 7.2 |
| 800 | 7.8 | 7.8 | 8.0 | 9.6 | 9.9 | 9.1 | 9.9 | 8.0 | 8.8 |
| 700 | 9.3 | 9.4 | 9.7 | 12.2 | 12.5 | 11.5 | 12.8 | 10.4 | 11.0 |
| 600 | 11.3 | 11.4 | 11.9 | 15.9 | 16.3 | 14.9 | 17.2 | 13.8 | 14.1 |
| $T_l$(°C) | 985.4 | 949.1 | 1001.5 | 1160.3 | 1194.9 | 1145.8 | 1234.7 | 1203.1 | 1126.6 |
| | Viscosities with 0 w.-% H2O | | | | | | | | |
| 1500 | 3.4 | 3.4 | 3.3 | 3.2 | 3.4 | 3.1 | 3.1 | 2.4 | 3.2 |
| 1400 | 4.0 | 4.0 | 3.9 | 3.9 | 4.1 | 3.8 | 3.8 | 3.0 | 3.9 |
| 1300 | 4.7 | 4.7 | 4.7 | 4.8 | 5.0 | 4.6 | 4.7 | 3.8 | 4.7 |
| 1200 | 5.5 | 5.5 | 5.5 | 5.8 | 6.1 | 5.6 | 5.7 | 4.7 | 5.6 |
| 1100 | 6.4 | 6.5 | 6.5 | 7.1 | 7.4 | 6.8 | 7.1 | 5.9 | 6.8 |
| 1000 | 7.6 | 7.6 | 7.7 | 8.7 | 9.1 | 8.4 | 8.8 | 7.4 | 8.3 |
| 900 | 9.1 | 9.1 | 9.3 | 10.9 | 11.3 | 10.5 | 11.2 | 9.4 | 10.2 |
| 800 | 10.9 | 10.9 | 11.3 | 14.0 | 14.4 | 13.3 | 14.6 | 12.2 | 12.8 |
| 700 | 13.3 | 13.3 | 13.9 | 18.5 | 19.0 | 17.4 | 19.8 | 16.4 | 16.5 |
| 600 | 16.6 | 16.6 | 17.6 | 26.1 | 26.6 | 24.1 | 28.9 | 23.4 | 22.2 |
| $T_l$(°C) | 1038.8 | 1047.1 | 1034.2 | 1179.4 | 1218.4 | 1167.2 | 1252.1 | 1266.4 | 1149.0 |

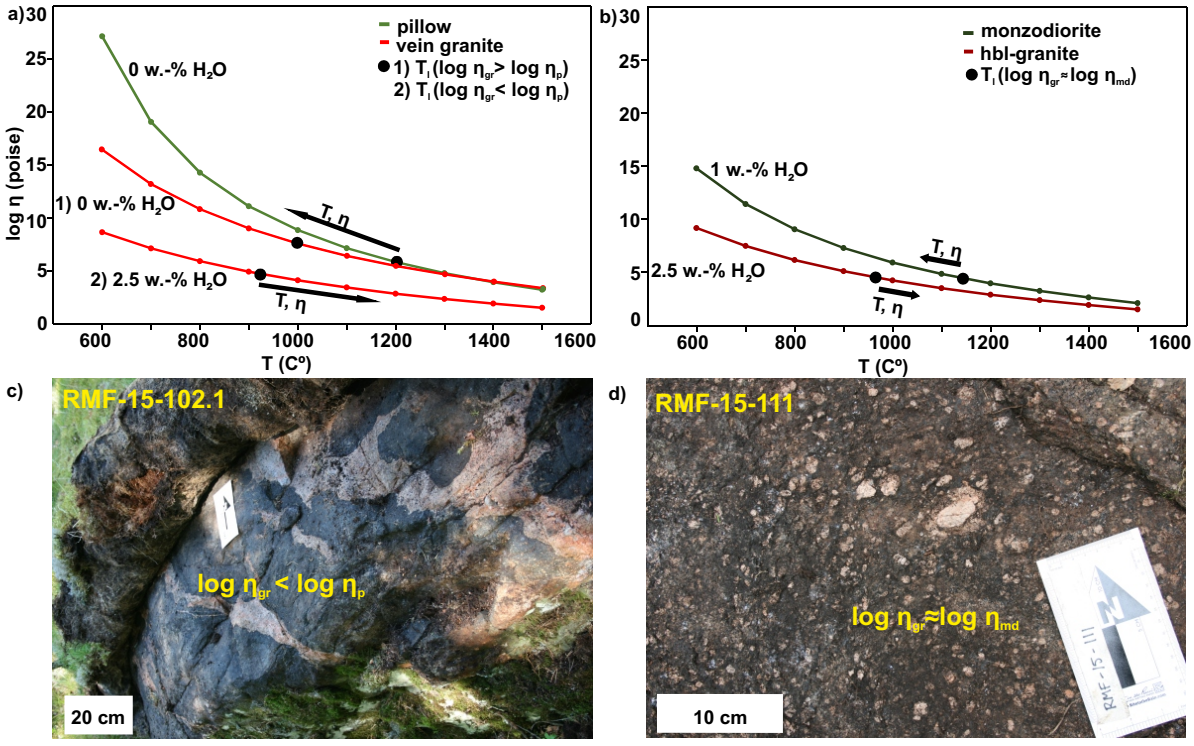


Figure 10. Melt viscosity (log η) curves calculated as a function of temperature (T) for a) monzodioritic pillows and granitic veins and b) massive monzodiorite and hbl-granite. Calculated liquidus temperatures of the magmas at the time of interaction and the resulting T/η-evolution of the components are shown as black dots and arrows, respectively. Outcrop photos showing the corresponding rock types and structures: c) mingled granitic and monzodioritic rocks and d) a mixed hybrid rock with monzodioritic groundmass and scattered alkali feldspar crystals.

The amount of $H_2O$ probably plays an important role concerning the viscosities of the two magmas, but the volatile content was not measured. Felsic melts most likely have higher $H_2O$ content, and the mafic melts are relatively drier, which would also affect the relative viscosities of the magmas at the time of interaction. Comparison of the viscosities of vein granites with 2.5 wt.% of $H_2O$ to pillows with 0 wt.% of $H_2O$, shows that the granite veins would naturally have lower viscosities (<5) at liquidus temperatures than the pillows (>5) (Fig. 10a), and no viscosity reversal would be required to explain the observations.

The water content of the mafic magma increases when the magma evolves, and the melt that produced the massive monzodiorites probably already had higher $H_2O$ content than the pillow magmas. Comparison of the massive monzodiorite with 1 wt.% of $H_2O$ to hbl-granite with 2.5 wt.% of $H_2O$ shows that their viscosities would have been similar at liquidus (Fig. 10b) enabling relatively efficient mixing of the two magmas.

The pillows most likely have reached thermal equilibrium with the hbl-granite rapidly, and the magmas had a too high viscosity difference to be able to mix. If the melts were relatively dry at thermal equilibrium the viscosities were more likely reversed. In this case, the mafic magma would have rapidly started to cool and crystallize forming pillows, and the granitic magma got superheated and less viscose and was able to intrude the monzodiorite as veins. However, the water content is considered to have affected the rheology as well. The amount of $H_2O$ increases when mafic magma evolves. The hbl-granite was superheated by the mafic magma, which led to loss of $H_2O$ to

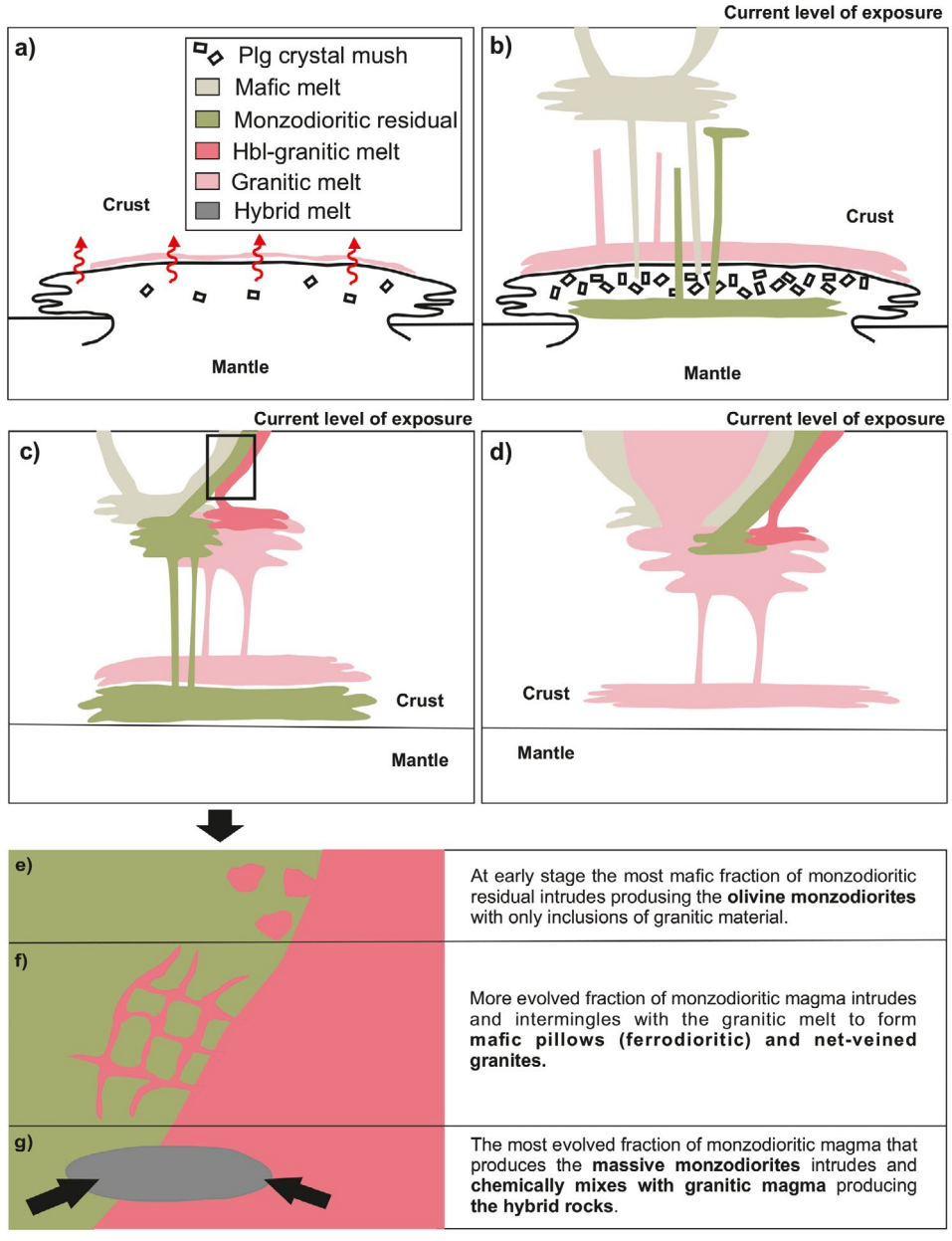


Figure 11. Schematic model of the magmatic evolution of the Ahvenisto complex by the classical two source model: a) the mantle-derived mafic magma ponds at the mantle-crust boundary, and starts to crystallize plagioclase and mafic minerals while heating the surrounding lower crust; b) the felsic magma is produced resulting from melting of the lower crust, and the anorthositic crystal mush intrudes into the upper crust forming an anorthositic arc and leaving behind a monzodioritic residual liquid; c) first fraction of a felsic melt (hbl-granitic) and monzodioritic residual liquid simultaneously intrude the cracks between the anorthositic arc and the country rocks, generating the different monzodiorite types and interaction styles at consequent stages; and d) finally the main granitic batholith is formed when the rest of the granitic magmas intrude the upper crustal levels producing the view seen in the current bedrock map (Fig. 2). e), f) and g) outlines the different interaction styles at different stages of the simultaneous intrusion of hbl-granite and monzodioritic magmas (the black rectangle in insert c).

the pillows. The $H_2O$ contribution from both of these effects probably in some cases compensated (monzodiorite vs. hbl-granite), and in others reversed and increased (pillows vs. granites) the relative viscosity difference of the two magmas. In the Ahvenisto complex, the water contents of the interacting magmas most likely played a more important role in the evolution of the mingling and mixing than other properties, such as composition and temperature.

### *7.4. Inferences for the magmatic evolution of the Ahvenisto complex*

Monzodioritic rocks are located between the bulk of anorthositic rocks and hbl-granite that is separate from the Ahvenisto main granite batholith. We have presented several evidence, which indicate that the monzodiorite and hbl-granite magmas behaved as liquids and intruded at the same time. The geochemical and mineralogical features that were described reveal that the monzodioritic rocks show a range of compositions as a result of differentiation, and that they have interacted with the hbl-granite magmas at several stages of their evolution. The structural location of these two rock types might suggest that they intruded into cracks between the already crystallized anorthositic rocks of the complex and the surrounding Svecofennian country rocks (Fig. 2 & 11). The sequence of intrusive events cannot be defined with the available information. Nevertheless, the results presented above suggest that the hbl-granite intruded first or simultaneously with the monzodiorite. This scenario is also supported by the arguments of Snyder and Tait (1995) and Wiebe (1996) according to which pillows form only when a basaltic magma intrudes a felsic magma reservoir, or in complex dykes in which the felsic magma is in contact with the country rocks and mafic pillows in the center.

We maintain that the classical two source model (Emslie et al., 1994, see also Rämö & Haapala 2005) can be applied to the formation of the Ahvenisto complex: A mantle derived mafic magma ponded at the mantle-crust boundary and fractionally crystallized plagioclase rich cumulates from which the anorthositic rocks formed, simultaneously heating the lower crust to produce the felsic partial melts parental to granitic rocks (Fig. 11a). The fractionation of the anorthosites left a monzodioritic residual liquid that intruded simultaneously with the first granitic melts (Fig. 11b & c). Finally, the main granitic batholith was formed when the larger more evolved fractions of granitic magma intruded (Fig. 11d).

Compositional variation in the monzodioritic rocks indicates that magmas may have intruded the crack at several stages (Fig. 11e,f & g). The evolution of the monzodioritic magma, and the proportions of mafic and felsic magma in each stage, might explain the variation in the observed interaction. The relative amount of basaltic magma would need to be high for it to be able to mix with a felsic magma (Sparks & Marshall, 1986). The olivine monzodiorite occurs only as a small local lens and it shows very little interaction with granite, only small enclaves of granitic material is found within it. This implies that only a small proportion of basaltic magma was injected. When the influx of more evolved monzodioritic magmabecame significant, the diminishing compositional and temperature contrast with the associated granitic melt, aided by the increasing water content in the monzodioritic magma, enabled the magmas first to mingle and finally to mix.

## 8. Conclusions

The evidence presented in this study suggest that the monzodioritic rocks in the Ahvenisto complex include a variety of types with contrasting mineral assemblages and geochemical composition that are related to fractional crystallization process of a mafic magma. Three types were identified: 1) olivine monzodiorite that has not been described in earlier studies; 2) ferrodiorite observed in mafic pillows; and 3) massive monzodiorite. Interaction with the hbl-granite has resulted in mingling and

mixing. Each monzodiorite type shows different style of interaction with the coeval granitic magma: in olivine monzodiorite the interaction is almost negligible; ferrodiorite is mingled with granite as mafic pillows and net-veined structures; and the massive monzodiorite has chemically mixed with hbl-granite to produce hybrid rocks. Compositional evolution of the mafic magma, together with the style and the timing of intrusion most likely controlled the interaction process. Interaction occurred at late stages in the evolution of the mafic arc, when the monzodioritic residual and hbl-granite were liquids simultaneously, and intruded into cracks between the anorthositic ring dyke and Svecofennian country rocks. Mafic-felsic melt interaction in the Ahvenisto complex area are clearly a more wide-spread phenomenon than previously thought, which makes Ahvenisto one of the key locations to study magmatic interaction processes.

## Acknowledgments

This study was made possible by funding granted to R.F. by the Doctoral school in natural sciences (DONASCI), Doctoral program in geosciences (GeoDoc), and the K.H. Renlund´s Foundation. The Authors acknowledge Dr. Saku Vuori for sharing his ideas and knowledge about the Tuuliniemi study area and hospitality during field work. We also thank Helena Korkka for the thin section preparations and Kirsi Larjamo for helpful discussions concerning petrography. Prof. Tapani Rämö gave his comments on an earlier version of the manuscript and Reijo Alviola provided invaluable information on the 1970's mapping projects that sparked the original idea for the study. Both are thanked for their crucial contributions. We acknowledge the reviewers Christophe Galerne and Shenghong Yang for their helpful and constructive comments and Arto Luttinen for his editorial efforts.

## *Supplementary data*

Electronic Appendices A–D for this article are available via Bulletin of the Geological Society of Finland web page.

## References

Alviola, R., Johanson, B.S., Rämö, O.T. & Vaasjoki, M., 1999. The Proterozoic Ahvenisto rapakivi granite-massif-type anorthosite complex, southeastern Finland; petrography and U-Pb chronology. Precambrian Research 95, 89–107. https://doi.org/10.1016/S0301-9268(98)00128-4

Ashwal, L. D., 1993. Anorthosites. Berlin. Springer, 422 p.

Bain, A.A., Jellinek, A.M. & Wiebe, R.A., 2013. Quantitative field constraints on the dynamics of silicic magma chamber rejuvenation and overturn. Contributions to Mineralogy and Petrology 165, 1275–1294. https://doi.org/10.1007/s00410-013-0858-5

Blake, D.H., Elwell, R.W.D., Gibson, I.L., Skelhorn, R.R. & Walker, G.P.L., 1965. Some relationships resulting from the intimate association of acid and basic magmas. Quaternary Journal of geological Society of London 121, 31–49.

Blundy, J.D. & Sparks, R.S.J., 1992. Petrogenesis of mafic inclusions in granitoids of the Adamello Massif, Italy. Journal of Petrology, 33, 1039–1104. https://doi.org/10.1093/petrology/33.5.1039

Boudreau, A.E. 1999. PELE- a version of the MELTS software program for the PC platform. Computers & Geosciences 25, 201–203. https://doi.org/10.1016/S0098-3004(98)00117-4

Campos, C.P.D., Perugini, D., Ertel-ingrish, W., Dingwell, D.B. & Poli, G., 2011. Enhancement of magma mixing efficiency by chaotic dynamics: an experimental study. Contributions to Mineralogy and Petrology 161, 863–881. https://doi.org/10.1007/s00410-010-0569-0

Chapman, M. & Rhodes, J.M., 1992. Composite layering in the Isle au Haut Igneous Complex Maine: evidence for periodic invasion of a mafic magma into an evolving magma reservoir. Journal of Volcanology and Geothermal Research 51, 41–60. https://doi.org/10.1016/0377-0273(92)90059-M

Duchesne, J.D., Liégeois, J.P., Vander Auwera, J. & Longhi, J., 1999. The crustal tongue melting model and the origin of massif anorthosites. Terra Nova 11, 100–105. https://.doi.org/10.1046/j.1365-3121.1999.00232.x

Emslie, R.F., 1978. Anorthosite massifs, rapakivi granites, and late Proterozoic rifting of North America. Precambrian Research 64, 273–288. https://doi.org/10.1016/0301-9268(78)90005-0

Emslie, R.F., 1991. Granitoids of rapakivi granite-anorthosite and related associations. Precambrian Research 51, 173–192. https://doi.org/10.1016/0301-9268(91)90100-O

Emslie, R.F., Hamilton, M.A., & Thériault, R.J., 1994. Petrogenesis of a Mid-Proterozoic anorthosite-mangerite-charnockite-granite (AMCG) complex: isotope and geochemical evidence from the Nain Plutonic suite. Journal of Geology 102, 539–558. https://doi.org/0022-1376/94/10205-007

Fourcade, S. & Allegre, C.J., 1981. Trace element behavior in granite genesis: a case study of the calc-alkaline plutonic association from the Querigut complex (Pyrenees, France). Contributions to Mineralogy and Petrology 76, 177–195. https://doi.org/0010-7999/81/0076/0177

Frost, C.D. & Frost, B.R., 1997. Reduced rapakivi-type granites: The tholeiite connection. Geology 25, 647–650. https://doi.org/10.1130/0091-7613

Frost, P.T. & Mahood, G.A., 1987. Field, chemical, and physical constraints on mafic-felsic magma interaction in the Lamarck Granodiorite, Sierra Nevada, California. Geological Society of America Bulletin 99, 272–291. https://doi.org/10.1130/0016-7606

Giordano, D., Russell, J.K. & Dingwell, D.B., 2008. Viscosity of magmatic liquids: A model. Earth and Planetary Science letters 271, 123–134. https://doi.org/10.1016/j.epsl.2008.03.038

Hall, A., 1996. Igneous Petrology. 2nd edition. London, Longman. 551 p.

Heinonen, A., 2012. Isotopic evidence for the origin of Proterozoic massif-type anorthosites and their relation to rapakivi granites in southern Finland and northern Brazil. Department of Geosciences and Geography, A18. Helsinki. Unigrafia.

Heinonen, A., Andersen, T. & Rämö, O.T., 2010a. Re-evaluation of rapakivi petrogenesis: Source constraints from the Hf isotope composition of zircon in the rapakivi granites and associated mafic rocks of southern Finland. Journal of Petrology 51, 1687–1709. https://doi.org/10.1093/petrology/egq035

Heinonen, A., Rämö, O.T., Mänttäri, I., Johanson B. & Alviola, R., 2010b. Formation and fractionation of High-Al tholeiitic magmas in the Ahvenisto rapakivi granite–massif-type anorthosite complex, southeastern Finland. The Canadian Mineralogist 48, 969–990. https://doi.org/10.3749/canmin.48.4.969

Heinonen, A., Andersen, T., Rämö, O.T. & Whitehouse, M.J., 2015. The source of Proterozoic anorthosite and rapakivi granite magmatism: evidence from combined *in situ* Hf-O isotopes of zircon in the Ahvenisto complex, southeastern Finland. Journal of the Geological Society 172, 103–112. https://doi.org/10.1144/jgs2014-013

Hibbard, M.J., 1995. Mixed magma rocks. Petrography to Petrogenesis, Prentice Hall 587, 242–257.

Hodge, K.F. & Jellinek, A.M., 2012. Linking enclave formation to magma rheology. Journal of Geophysical Research 117, 1–12. https://doi.org/10.1029/2012JB009393

Hodge, K.F., Carazzo, G. & Jellinek, A.M., 2012. Experimental constraints on the deformation and breakup of injected magma. Earth and Planetary Science Letters 325–326, 52–62. https://doi.org/10.1016/j.epsl.2012.01.031

Huppert, H.E. & Sparks, R.S.J., 1988. The generation of Granitic magmas by intrusion of Basalt into Continental Crust. Journal of Petrology 29, 599–624. https://doi.org/10.1093/petrology/29.3.599

Johanson, B.S., 1984. Ahvenisto gabbro-anortositkomplex- En petrografisk och mineralogisk undersökning. Helsingfors universitet, Helsinki, Finland.

Katzir, Y., Litvinovsky, B.A., Jahn, B.M., Eyal, M., Zanvilavich, A.N., Valley, J.W., Vapnik, Ye., Beeri, Y. & Spicuzza, M.J., 2007. Interrelations between coeval mafic and A-type silicic magmas from composite dykes in a bimodal suite of southern Israel, noerthernmost Arabian-Nubian Shield: Gheocemical and isotope constraints. Lithos 97, 336–364. https://doi.org/10.1016/j.lithos.2007.01.004

Kivisaari, H., 2015. High-aluminum orthopyroxene megacrysts (HAOM) and the polybaric crystallization of the Ahvenisto anorthosite. Unpublished MSc thesis, Department of Geosciences and Geography, University of Helsinki, 64 p.

Litvinovsky, B.A., Zanvilevich, A.N., Wickham, S.M., Jahn, B.M., Vapnik, Y., Kanakin, S.V. & Karmanov, N.S., 2017. Composite dikes in four successive granitoid suites from Transbaikalia, Russia: The effect of silicic and mafic magma interaction on the chemical featyures of granitoids. Journal of Asian Earth Sciences 136, 16–39. https://doi.org/10.1016/j.jseaes.2016.12.037

Marshall, L.A. & Sparks, R.S.J., 1984. Origin of some mixed-magma and net-veined ring intrusions. Journal of Geological Society 141, 171–182. https://doi.org/10.1144/gsjgs.141.1.0171

Padilla, A.J., Miller, C.F., Carley, T.L., Economos, R.C., Schmitt, A.K., Coble, M.A., Wooden, J.L., Fisher, C.M., Vervoort, J.D. & Hanchar, J.M., 2016. Elucidating the magmatic history of the Austurhorn silicic intrusive complex (southeast Iceland) using zircon elemental and isotopic geochemistry and geochronology. Contributions to Mineralogy and Petrology 171, 1–21. https://doi.org/10.1007/s00410-016-1279-z

Rämö, O.T. & Haapala, I., 2005. Rapakivi granites. In Lehtinen, M., Nurmi, P.A. & Rämö, O.T. (eds.), Precambrian Geology of Finland – Key to the evolution of the Fennoscandian Shield. Elsevier, Amsterdam, pp. 533–562. https://doi.org/10.1016/S0166-2635(05)80013-1

Salonsaari, P.T., 1995. Hybridization in the subvolcanic Jaala-Iitti complex and its petrogenetic relation to rapakivi granites and associated mafic rocks of southeastern Finland. Bulletin of the Geological Society of Finland 67, 104 p.
https://doi.org/10.17741/bgsf/67.1b

Savolahti, A., 1956. The Ahvenisto massif in Finland, The age of the surrounding gabbro-anorthosite complex and the crystallization of the rapakivi. Bulletin de la Comissione Geologique de Finlande 174.

Savolahti, A., 1966. The differentiation of gabbro-anorthosite intrusions and the formation of anorthosites. Comptes Rendus de la Societe Geologique de Finlande 38, 173–197.

Snyder, D. & Tait, S., 1995. Replenishment of magma chambers: comparison of fluid-mechanic experiments with field relations. Contributions to Mineralogy and Petrology 122, 230–240.
https://doi.org/10.1007/s004100050123

Snyder, D., Granbes, C., Tait. S. & Wiebe, R.A., 1997. Magma Mingling in Dikes and Sills. The Journal of Geology 105, 75–86.
https://doi.org/10.1086/606148

Sparks, R.S.J. & Marshall, L.A., 1986. Thermal and mechanical constraints on mixing between mafic and silicic magmas. Journal of volcanology and Geothermal Research 29, 99–124.
https://doi.org/10.1016/0377-0273(86)90041-7

Walker, G.P.L. & Skelhorn, R.R., 1966. Some associations of acid and basic igneous rocks. Earth-Science Reviews 2, 93–109.
https://doi.org/10.1016/0012-8252(66)90024-9

Weidendorfer, D., Mattsson, H.B. & Ulmer, P., 2014. Dynamics of Magma Mixing in Partially Crystallized Magma Chambers: Textural and Petrological Constraints from the Basal Complex of the Austurhorn Intrusion (SE Iceland). Journal of Petrology 55, 1865–1903.
https://doi.org/10.1093/petrology/egu044

Wiebe, R.A., 1987. Structural and Magmatic Evolution of a Magma Chamber: The Newark Island Layered Intrusion, Nain, Labrador. Journal of Petrology 29, 383–411.
https://doi.org/10.1093/petrology/29.2.383

Wiebe, R.A., 1991. Commingling of contrasted magmas and generation of mafic enclaves in granitic rocks. In: Didier, J. & Barbarin, B. (eds.), Enclaves and Granite Petrology, Developments in Petrology 13. Amsterdam. Elsevier, pp. 393–402.

Wiebe, R.A., 1993. The Pleasant Bay Layered Gabbro-Diorite, Coastal Maine: Ponding and Crystallization of Basaltic Injections into a Silicic Magma Chamber. Journal of Petrology 34, 461–489.
https://doi.org/10.1093/petrology/34.3.461

Wiebe, R.A., 1996. Mafic-silicic layered intrusions: the role of basaltic injections on magmatic processes and the evolution of silisic magma chambers. Transactions of the Royal Society of Edinburgh: Earth Sciences 87, 233–242.
https://doi.org/10.1130/0-8137-2315-9.233

Wiebe, R.A. & Ulrich, R., 1997. Origin of composite dikes in the Gouldsboro granite, coastal Maine. Lithos 40, 157–178.
https://doi.org/10.1016/S0024-4937(97)00008-X

Wiebe, R.A., Frey, H. & Hawkins, D.P., 2001. Basaltic pillow mounds in the Vinalhaven intrusion, Maine. Journal of Volcanology and Geothermal Research 107, 171–184.
https://doi.org/10.1016/S0377-0273(00)00253-5